Energy Conversion and Management 112 (2016) 288–307

Contents lists available at ScienceDirect

Energy Conversion and Management

journal homepage: www.elsevier.com/locate/enconman

Multi-agent based distributed control architecture for microgrid energy management and optimization

M. Reyasudin Basir Khan *, Razali Jidin, Jagadeesh Pasupuleti

College of Engineering, Universiti Tenaga Nasional, Jalan IKRAM – UNITEN, 43000 Kajang, Selangor, Malaysia

ARTICLE INFO

Article history:
Received 11 November 2015
Accepted 7 January 2016

Keywords:
Multi-agent
Energy management system
Microgrid
Renewable energy system
Game-theory

ABSTRACT

Most energy management systems are based on a centralized controller that is difficult to satisfy criteria such as fault tolerance and adaptability. Therefore, a new multi-agent based distributed energy management system architecture is proposed in this paper. The distributed generation system is composed of several distributed energy resources and a group of loads. A multi-agent system based decentralized control architecture was developed in order to provide control for the complex energy management of the distributed generation system. Then, non-cooperative game theory was used for the multi-agent coordination in the system. The distributed generation system was assessed by simulation under renewable resource fluctuations, seasonal load demand and grid disturbances. The simulation results show that the implementation of the new energy management system proved to provide more robust and high performance controls than conventional centralized energy management systems.

1. Introduction

Widespread integration of distributed multi-source generators pose a challenge to the present electrical grid system. More integration of renewable energy (RE) generation systems into the present distribution networks adds new dynamic elements due to the intermittencies and inherent unpredictability of the renewable energy system (RES) operations. Therefore, in order to improve the present performance of such systems, it is crucial for the energy management system (EMS) to have an effective and optimal control strategy. The EMS should primarily be able to provide balance between the electricity supply and load demand. Additionally, the system must also comply with other requirements such as reliability, flexibility, fault tolerance and operating costs reduction.

Typically, most energy management systems are based on centralized controllers. For instance, a generic centralized EMS utilized for managing power converters in a microgrid that consists of wind and Photovoltaic (PV) systems as described in [1]. In [2], the centralized EMS was used to coordinate the micro-generators with the main grid for minimizing the greenhouse gases (GHG) emissions, energy costs, and maximizing the power output of renewable energy systems. Furthermore, in [3], a microgrid central controller was used to optimize supply and demand profiles for mitigating fuel consumption costs.

Conventional EMS architecture is summarized in Fig. 1. The central supervisory controller is used to optimize the usage of fossil fuel based distributed energy resources (DERs), renewable DERs, and energy storage in the microgrid. It commonly consists of a communication network that monitors the DERs and also sends commands to local controllers in order for the dispatchable resources to deliver power to the load in the most promising economical method. Despite its universal successes, this system's top-down approach has several drawbacks. It represents a 'single point of failure', which means that it has to be securely planned with proper redundancy built in [1,4]. In addition, the complexity of the centralized energy management system grows exponentially with the growing number of generators and loads causing the higher cost of communication for scheduling and online monitoring [5,6]. Moreover, the centralized controller needs to be updated and reconfigured for any changes in the microgrid structure or when new generators or loads are installed [6]. Although centralized control methods may be used to find the best control solutions, it require powerful computing ability in order to deal with a huge amount of data as the systems become bigger and more complex [6]. It also needs a network with a highly distributed control strategy and communication capabilities [7].

On the other hand, decentralized control based on a bottom-up approach for energy management systems is more robust and less complex than centralized management [8,9]. The distributed

* Corresponding author. Tel.: +603 8921 2020; fax: +60 3 8928 7166.
E-mail addresses: Reyasudin@uniten.edu.my, reyasudin@gmail.com (M.R. Basir Khan), Razali@uniten.edu.my (R. Jidin), Jagadeesh@uniten.edu.my (J. Pasupuleti).

http://dx.doi.org/10.1016/j.enconman.2016.01.011
0196-8904/

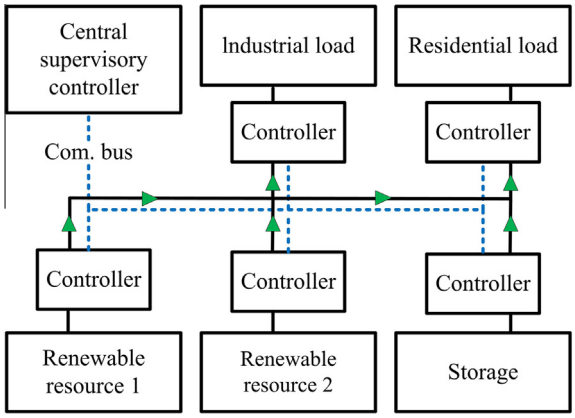

Fig. 1. Typical centralized EMS for distributed generation system [10].

management components are viewed as a unit with some intelligence that enables them to provide basic computation, planning action and decision-making. It not only minimizes the communication and computation capability; but also completely respects other various parts requirements and operational performance [7]. Therefore, it is expected that an intelligent, dynamic and open system that is self-adaptive is essential in order for the hybrid RE system to function effectively under various conditions to meet dynamic load variations and renewable sources intermittency. This paper focuses on multi-agent system (MAS) based EMS architecture for optimizing hybrid RE system performance.

Extensive research has been conducted on energy management for micro-grids and distributed generation. Many researchers have implemented a hierarchical control structure for controlling microgrid and distributed generations. In [11], a hierarchical EMS was used to control a microgrid that includes three control layers such as supervisory, optimizing and execution. In addition, a hierarchical EMS comprised of master and slave control strategy was used in [12] to control a microgrid composed of PV, wind, hydrogen and battery system. There were also several energy management methods utilizing soft-computing approaches to control the microgrid such as genetic algorithm, fuzzy logic, particle swarm optimization, and neural networks. For instance, a genetic algorithm based EMS employed to manage and optimize the generation dispatch of a microgrid with multiple generators was presented in [13]. Meanwhile in [14], fuzzy logic EMS was used to optimize the operation of microgrid components and sizes. In [15], particle swarm optimization was used in the EMS to optimize the power output between the distributed generators aiming to improve the power quality in the microgrid. Moreover, in [16], a neural network based EMS applied in the PV microgrid to optimally manages the system's operation by adapting to the input variable such as PV output power and load demand.

MASs have been widely studied in the field of computer science [17]. However, in recent years, the development of the MAS has gained attention from power system researchers for application in the field of hybrid energy systems and microgrids for distributed control and energy management [7,18]. A multi-agent system for optimizing the hybrid RE system was presented in [7]. Meanwhile in [18], a distributed management solution based on MAS was proposed to provide better system reliability than conventional centralized EMS. In [9], a MAS based hierarchical decentralized coordinated control was presented to solve the energy management issue of a distributed generation system (DGS) by ensuring energy supply with high security. A MAS and fuzzy cognitive map were used in [8] for a decentralized energy management system of an autonomous poly-generation microgrid. In [19], a decentralized MAS was used for demand side integration that was able to reduce the energy cost, improve energy efficiency and increase security and quality of supply. Furthermore, MAS has also been used for reactive power management in distribution networks with renewable energy sources to enhance the dynamic voltage stability [20].

All the mentioned researchers concluded that the MAS-based decentralized energy management control structure is capable of handling complex DGS or hybrid energy systems more effectively, since it can deliver several key advantages to the system [8,9,18,21]. Firstly, one of the major advantages is the high reliability and robustness of the system. For instance, if one of the controllers fails, the rest of the system can still operate in part, and it does not affect the entire system's performance. As such, the managed microgrid has a higher likelihood of partial operation in cases when malfunctions take place in different parts of the system. Moreover, the MAS DGS also offers flexibility since the different levels of agents not only can identify and respond quickly to the environmental variations, but also depend on each other to regulate the operational status in reaction to the changes. The MAS based distributed scheme is also more feasible to handle than a centralized scheme. The agents are not only able to strategize their own asynchronous decision-making simultaneously, but can also attain the goal of the whole system in a cooperative way. The MAS can also minimize the communication and computation burden since the dynamic information, basic computation, action-planning and decision making can be processed by individual agents locally. Finally, the openness and adaptability of the MAS-based energy management system allows the integration of new DER units or loads without reconfiguring the entire system. Therefore, in this paper, a new MAS based decentralized control architecture was implemented for a microgrid in order to handle the complex energy management issue of the DGS.

The remaining sections of this paper are organized as follows: In Section 2, the MAS concept such as the definition, agent's characteristics and the MAS contributions for the EMS are presented. Moreover, details of the distributed generation model that comprises of components such as diesel generator, PV system, wind system, micro-hydropower system, battery storage system, and loads are included in Section 3. The utilization of MAS in the microgrid with agent model for each component, MAS architecture and global objective function are shown in Section 4. The game theory implementation for multi-agent coordination in the microgrid is described in Section 5. Meanwhile, the simulation and results of this paper that includes the case study, performance evaluations through different scenarios, and comparison with a centralized system are discussed in Section 6. Finally, Section 7 presents the conclusions of this paper.

2. Multi-agent systems concept

2.1. Multi-agent systems

MAS is one of the domains in agent based technology that deals with modeling of independent or autonomous decision-making units [17]. It is comprised of a group of agents that are able to interact with each other [22]. The MAS method is rarely used in the electrical engineering field. Undeniably, the use of MASs offers difficulties in the electrical engineering area which includes the broad collection of design practices, variety of agent structures, and various methods of implementation [23,24]. MAS EMS for a microgrid is among the preferred options for implementation of an intelligent power system, where each essential component is represented by an intelligent autonomous agent. Therefore, in this paper, the microgrid system's power generations, consumer loads,

and all other components in the network are monitored and controlled by an autonomous agent with a common communication bus.

2.2. Agents

There is no universally agreed-upon definition on what an agent is [18,25]. However, an agent generally means a computer system that is placed in an environment that is capable of performing autonomous actions in this environment in order to achieve its design objectives [25]. An agent also can be viewed as a system that is able to perceive its environment through sensors and act upon that environment by means of actuators [22,26]. So, an agent is typically represented by any control system. However, an intelligent agent is defined as an agent capable of doing flexible autonomous action in order to achieve its design objectives [25]. It has three key features namely reactive, proactive and social abilities [23,25,27]. Reactivity is the ability of the agent to perceive the environment and react to any changes. Pro-activeness is the intelligent agent's ability to display goal-directed performance. Lastly, the intelligent agent's social ability is its capability to interact with other agents either in a cooperative or competitive manner. All the agent's characteristics tend toward achieving its design objectives by taking into consideration its available resources and skills, and also rely on its perception, communications, and representations.

From its characteristics, the agent technology is promising for the implementation of flexible, scalable, and distributed systems. Thus, MAS is capable of solving many problems faced by the centralized energy management system.

2.3. MAS for energy management

This paper focuses on the use of an MAS in order to optimize the hybrid renewable energy system's performance. The hybrid renewable energy system is comprised of PV systems, wind turbines, battery storage systems, micro-hydropower systems, and diesel generators.

The proposed MAS based EMS will be able to provide the following solutions to the microgrid system:

1. coordination mechanism and communication protocol for all elements in the microgrid,
2. control schemes based on the output characteristics of various types of power sources,
3. control strategy to optimize the trade-off between the system's performance and operation cost,
4. optimization of the microgrid system's operation considering load demand and intermittency of RE resources, and
5. optimal usage of each component in the microgrid.

3. Distributed hybrid RE generation system

3.1. Systems' architecture

The overview of a microgrid implemented with an MAS based energy management system is shown in Fig. 2. The system comprises of PV systems, wind turbines, battery storage systems, micro-hydropower systems, and diesel generators. The distributed control system manages and optimizes the output of each power

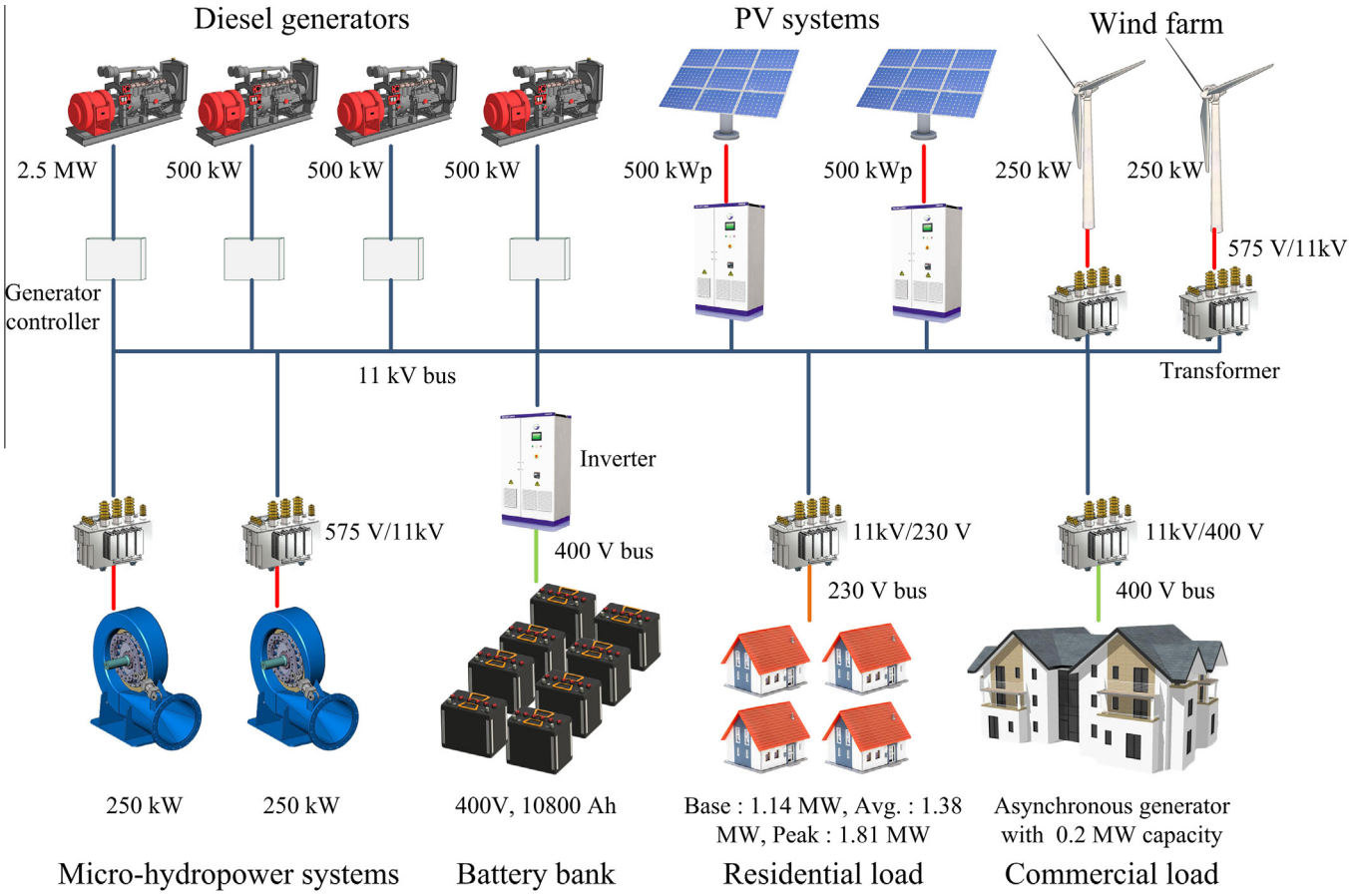

Fig. 2. Microgrid schematic.

generation system based on the load demand and available RE resources. Hence it will provide an optimal and stable grid-connected operation of the power generation units.

3.2. Modeling of distributed generation system

The system-level microgrid model that consists of distributed generation systems was developed, simulated, and tested using Simulink SimPowerSystems. The microgrid consists of six key components: diesel generators, PV, wind farms, micro-hydropower systems, battery storage system and loads of the grid. The diesel generator will provide base power for the microgrid. Meanwhile, there are three types of renewable energy system consisting of PV systems, wind turbines and micro-hydropower systems connected to the grid. Due to the complexity of the network, the microgrid model is simulated using SimPowerSystem's phasor mode in order to perform a faster simulation time for a 24 h scenario. The Simulink model of the microgrid is shown in Fig. 3.

As shown in Fig. 3, the grounding transformer was utilized in the model's utility distribution networks in order to provide a neutral point in the three-wire system. Meanwhile, the two small resistive loads connected at the machine terminal and distribution networks are used to avoid numerical oscillation in the model.

3.2.1. Microgrid structure and electrical network

The microgrid is a standalone PV–wind–hydro–diesel-battery system with a capacity of 6 MW. The renewable energy contributed 2 MW to the total energy capacity. The system is comprised of four diesel generators: one 2.5 MW diesel generator, and three diesel generators with rated capacity of 500 kW each. Meanwhile, the PV system consists of two 500 kWp PV arrays. The wind farm consists of two wind turbines, each with a rated capacity of 250 kW. The micro-hydropower plant with a run-of-river scheme is modeled with two turbines with a rated capacity of 250 kW each. The battery storage system is used to reduce the power production from diesel generators. In this system, the 2.5 MW diesel generator operates as a base station, with its output supplemented by the three 500 kW diesel sets.

The battery is controlled based on the load following dispatch strategy where only renewable energy systems will charge the battery, not the diesel generators. The grid will feed energy from PV, wind and micro-hydropower systems that are connected at AC distribution line in day time. This energy will be used directly to supply the load; meanwhile the surplus energy will be used to charge the battery storage system. The secondary load bank is activated when the battery system is fully charged for dumping the surplus energy produced by the RE systems. The diesel generators will also be started during day time if the total renewable energy capacity cannot supply enough power to the load.

During night time, if the RE system configurations cannot cater power for the load demand, the batteries will be used to supply energy to the loads. When, the total load demand is higher than the battery capacity or the batteries have been fully discharged, then, the diesel generators will be turned on.

The electrical system network consists of an 11 kV, 50 Hz distribution network. The power generation systems, such as PV, wind, micro-hydro and diesel systems are AC linked to the grid. The diesel generator and PV system are directly connected to the 11 kV bus. Meanwhile, the grid consists of a 575 V bus at the wind farm and micro-hydropower systems which is stepped up from 575 V to

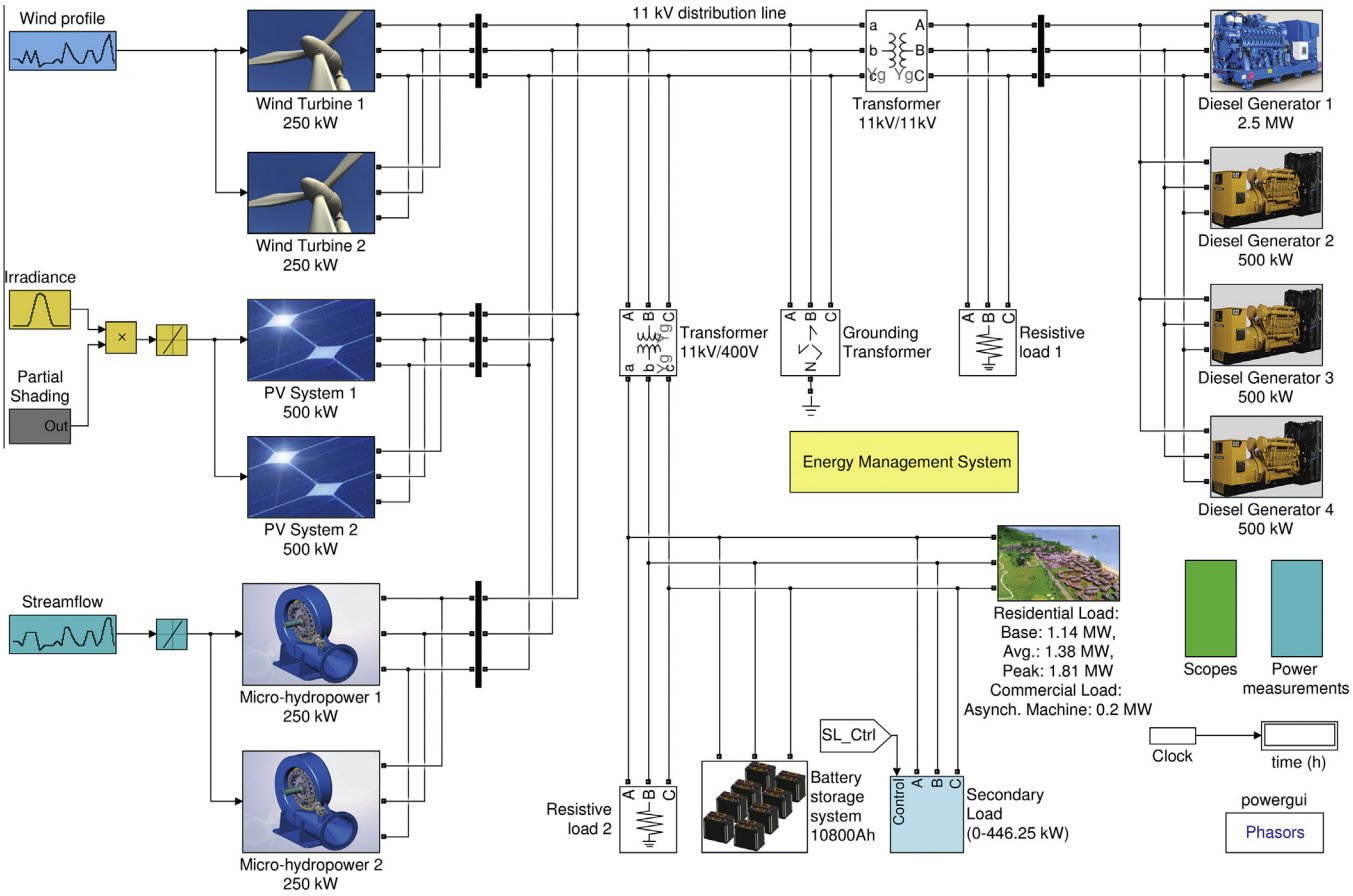

Fig. 3. Simulink model of the microgrid.

11 kV for distribution. Then, the 11 kV is stepped down to 230 V and 400 V for residential and commercial three phase loads, respectively. The single phase loads were not modeled in this system. The modeled residential load has a base power of 1.14 MW, average power of 1.38 MW and peak power of 1.81 MW. Meanwhile, the industrial load modeled using asynchronous machine with capacity of 0.2 MW.

3.2.2. Diesel generator

The diesel generator provides balance to the generated power and load demand in the microgrid. The model comprises of a diesel engine, governor, excitation system and synchronous machine. The diesel engine and governor system model are combined into one block which has two inputs which are the desired and actual speed (in p.u.). The output of the block is the diesel engine mechanical power. The controller is modeled as the following transfer function [28]:

$$H_c = \frac{k(1+T_3 s)}{1+T_1 s+T_1 T_2 s^2} \tag{1}$$

where k is the proportional gain and T_1, T_2 and T_3 are the regulator time constants (seconds). The actuator transfer function is as follows [28]:

$$H_a = \frac{1+T_4 s}{[s(1+T_5 s)(1+T_6 s)]} \tag{2}$$

where T_4, T_5 and T_6 are the actuator time constants (seconds). Meanwhile, the diesel engine generator is modeled as a time delay by delaying the torque output form the actuators in a specified amount of time.

The excitation system for the synchronous machine is represented by the following transfer function [28]:

$$\frac{V_{fd}}{V_{ro}} = \frac{1}{K_s + sT_e} \tag{3}$$

where V_{fd} is the exciter voltage, V_{ro} is the regulator's output, K_s is the gain and T_e is the time constant (seconds). The synchronous machine is modeled using the SimPowerSystems's three phase synchronous machine block operating in generator mode.

3.2.3. PV system

The energy produced by the PV arrays are proportional to three elements: the solar radiation data, the PV panel's efficiency and the PV system area size. The PV power output relationship with irradiance, efficiency and area size are modeled as follows [28–30]:

$$P_{PV} = GF_P A_{PV} e_{pv} \tag{4}$$

where P_{PV} is power output from PV farm (kW), G is the irradiance (W/m^2), F_P is partial shading factor (fixed at 0.7), A_{PV} is the area covered by the PV farm (m^2) and e_{pv} is the efficiency factor (assumed as 0.1). The PV system modeled based on the typical monocrystalline modules.

3.2.4. Wind turbine

The wind turbine model generates electrical power according to the linear relationship with the wind speed. The simplified wind turbine is modeled such that the power output from the wind turbine varies as a cube of the wind speed. The wind turbine will produce nominal power when the wind speed has nominal value. However, when the wind speed surpasses the maximum wind speed value, the wind turbine will disconnect from the grid until the wind speed returns back to its nominal value. The wind turbine model is represented as follows [28,30]:

$$P_W = \begin{cases} v^3 \cdot \frac{P_{nom}}{v_{nom}} & (v \leqslant v_{nom}) \\ v_{nom}^3 \cdot \frac{P_{nom}}{v_{nom}} & (v_{nom} \leqslant v < v_{\max}) \\ 0 & (v \geqslant v_{\max}) \end{cases} \tag{5}$$

where P_W is the wind turbine output power (kW), P_{nom} is the nominal power (kW), v is the wind speed (m/s), v_{nom} is the nominal wind speed (m/s) and $v_{\max}$ is the maximum wind speed (m/s).

3.2.5. Micro-hydropower system

The micro-hydropower system's electrical power output is directly proportional to the turbine characteristics and streamflow as shown in the following equation [31–33]:

$$P_m = \rho q h g e_h \tag{6}$$

where P_m is the power output from turbine (W), ρ is water density (1000 kg/m^3), q is water flow (m^3/s), h is gross head height (m), g is acceleration of gravity (9.81 m/s^2), and e_h is the efficiency factor (fixed at 0.7). At low streamflow, the micro-hydropower system, together with diesel generator, PV system, and wind farm are required to feed the load. The secondary load bank will be activated when the battery system is fully charged for dumping the excess energy produced by the RE systems.

3.2.6. Battery storage system

The battery storage system stores the surplus energy generated by the renewable energy power generation systems. However, the battery bank will be discharged in order to meet the load demand when there is a power shortage from the renewable energy generation systems. The batteries' simple dynamics are modeled as follows [28,30,34]:

$$\mathrm{SOC}_{bat} = 100\left[1 - \left(\frac{1}{Q_{bat}} \cdot \int_0^t i_{bat}\ (t)dt\right)\right] \tag{7}$$

$$B_{AH} = \frac{1}{3600}\int_0^t i_{bat}(t)\ dt \tag{8}$$

where SOC_{bat} is the battery state of charge (%), Q_{bat} is the maximum battery capacity (A h), i_{bat} is the battery current and B_{AH} is the battery ampere-hour. The battery's initial state-of-charge (SOC) is set to 80%. In this system, the battery is modeled according to the characteristics of deep cycle lead acid batteries with discharge efficiency assumed to be 90%.

3.2.7. Load

The load is comprised of both residential and commercial loads. The commercial load is denoted by an asynchronous machine in order to represent the impact of commercial inductive load, such as an air conditioning system, on the microgrid. The residential load is modeled according to the daily consumption profile in non-monsoon seasons of a resort island that are further explained in Section 6.1. The residential load was simulated according to the real variation of daily load profile of a selected resort island. The modeled residential load has a base power of 1.14 MW, average power of 1.38 MW and peak power of 1.81 MW. Meanwhile, the industrial load modeled using asynchronous machine with capacity of 0.2 MW.

3.2.8. Secondary load

The secondary load is designed to absorb the excess power generated by the RE system when the battery system is fully charged. It is comprised of eight sets of three-phase resistors connected in series where the nominal power of each set follows a binary progression in order for the load to be varied from 0 to 446.25 kW by steps of 1.75 kW.

4. MAS utilization for energy management

This system utilizes the distributed artificial intelligence technology which is built based on a bottom-to-top approach in order to satisfy the requirements of adaptability, openness, autonomous, and fault tolerance of the microgrid system.

The energy management Simulink block in Fig. 3 is comprised of the complete implemented EMS. The EMS objective is to make decisions for reconfiguring and optimizing the system based on the environmental and system parameter variations in order to fulfil the load demand. The EMS also will make decisions to optimize the system's efficiency and benefits. Furthermore, it will assess the microgrid performance according to the optimal usage of the multiple power generation systems.

The reorganization and optimization excitation mechanism is excited by the microgrid from the variation of renewable resources, load demand, and output power. When the reorganization is activated, the decisions are being made by the EMS considering the consumer demand, renewable resource data, energy cost and the agent's mode.

The main power contributors to the grid are renewable energy systems. Each renewable power source depends on its own renewable source which is highly intermittent, therefore having unstable power output throughout the day. The agent for each component must have some intelligence in order to monitor the changes in the systems and make decisions locally.

Moreover, the design of the global objective function will consider many factors such as agent modes, energy cost, power outputs, power losses and load demand. Conversely, the decision of each agent locally will contribute in attaining optimization goals for the whole system.

4.1. EMS agent models

The agent's structure was modeled in Simulink SimPowerSystems whereas its behavior was modeled using Simulink Stateflow. This paper focuses on the feasibility of a multi-agent system for a decentralized energy system in a simulation environment. Therefore, JADE (Java Agent Development Framework) or any other agent software was not used in designing the multi-agent systems.

The intelligent agents are constructed based on layered architectures where the agent's control subsystems are arranged hierarchically by increasing the level of abstraction of information interpretation at higher levels of layers.

In this system, the agent's architecture has been modeled based on InteRRaP that has a vertical layering structure with two pass controls [35]. The InteRRaP has been used widely in the robotics field [36]. However, in this study, the InteRRaP architecture has been modified in order to suit its application in the power system field for modeling agents in the microgrid environment. The modified agent architecture is shown in Fig. 4.

The sensors' input is passed through one higher layer at a time and flows back to the lower level of the architecture to generate the action output for the actuator. The detailed information for each layer is shown in Table 1. For this system, there are eight types of agents used for controlling and monitoring each component of the microgrid. Each agent has its own structure for controls and handling information.

This paper presents a new architecture for MAS modeling in microgrid for EMS. The agent model comprise of two control cycles where it will sense, identify, plan, cooperate, decide and act in one cycle. Meanwhile, it will control and learn in another cycle. However, in this paper, the agent learning process will not be covered.

4.1.1. PV agents (PAs)

The PV system is represented by an agent. It will monitor the irradiance and also the performance and total power generated by the PV system.

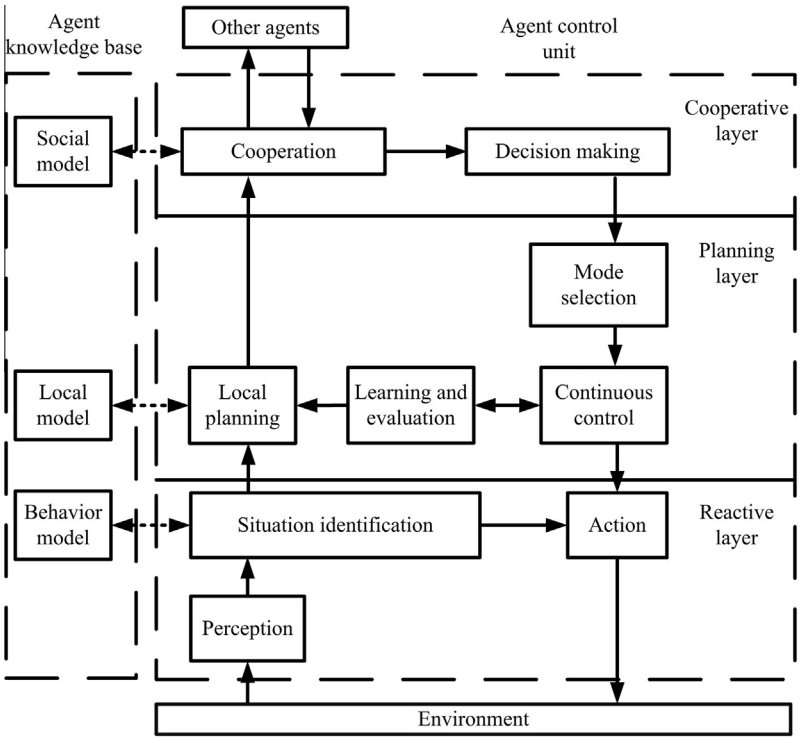

Fig. 4. Agent architecture.

Table 1
Agent layers descriptions.

Description	Layer		
	Reactive	Planning	Cooperative
Input	(a) Meteorological data (solar irradiance, wind speed, streamflow), battery SOC (b) Restructuring instruction	(a) Mode parameters	(a) Mode (b) Output capability (c) Performance index (d) Power cost
Process	(a) Mode assessment (b) Mode comparison	(a) Output capability computation (b) Decision making (c) Learning and evaluation (d) Dynamic control	(a) Cooperation request (b) Decision making
Output	(a) To planning layer: Mode, meteorological parameters (b) To action: Perform action, execute restructuring	(a) To cooperative layer: mode, output capability, performance index, power cost (b) To reactive layer: Decision	(a) To other agents/EMS: Mode, output capability, performance index, power cost (b) To planning layer: Overall decision

4.1.2. Wind farm agents (WAs)

The wind energy conversion system (WECS) is represented by an agent. This agent will monitor the wind speed alongside the performance and total power generated by the wind turbines.

4.1.3. Micro-hydropower agents (MAs)

The micro-hydropower system is represented by an agent. This agent will monitor the streamflow together with the performance and total power generated by the micro-hydropower systems.

4.1.4. Diesel generator agents (DAs)

The diesel generators connected to the grid are represented by an agent. It will take inputs from total renewable energy power output, battery SOC and load demand in order to turn on the necessary diesel generators to supply electricity for consumers. The 2.5 MW diesel generator will be providing the base power while its output is supplemented by the three 500 kW diesel generators. This agent will use the surplus load demand for selecting and determining the total diesel generation capacity as represented by the following expressions:

$$P_D = \begin{cases} P_{d1}+P_{d2}+P_{d3}+P_{d4} & \Delta P_L \geqslant P_{d1,\max}+P_{d2,\max}+P_{d3,\max} \\ P_{d1}+P_{d2}+P_{d3} & P_{d1,\max}+P_{d2,\max} \leqslant \Delta P_L < P_{d1,\max}+P_{d2,\max}+P_{d3,\max} \\ P_{d1}+P_{d2} & P_{d1,\max} \leqslant \Delta P_L < P_{d1,\max}+P_{d2,\max} \\ P_{d1} & \Delta P_L < P_{d1,\max} \\ 0 & \Delta P_L = 0 \end{cases} \tag{9}$$

where P_D is the total diesel generation capacity (kW), ΔP_L is the surplus consumer load need to be satisfied, meanwhile P_{d1}, $P_{d2,}$ P_{d3} and P_{d4} are the capacity for each diesel generators in the system (kW), and $P_{d1,\max}$, $P_{d2,\max}$, $P_{d3,\max}$ and $P_{d4,\max}$ are the maximal capacity of each diesel generators. In order to increase the lifetime of the diesel generator sets, the generators daily total of startup and shutdown constraint was introduced as follows:

$$N_{startup} \leqslant N_{startup,\max}, N_{shutdown} \leqslant N_{shutdown,\max} \tag{10}$$

where $N_{startup}$ is the number of startup, $N_{startup,\max}$ is the maximum number of startup, $N_{shutdown}$ is the number of shutdown and $N_{shutdown,\max}$ is the maximum number of shutdown. The generation constraint was also introduced to make sure the generators operated within lower and upper limits. The diesel generators' operating zones' constraints are represented as follows:

$$P_{di,\min} \leqslant P_{di} \leqslant P_{di,\max} \tag{11}$$

where P_{di} is the active power for generator i, $P_{di,\min}$ is the minimum active power output of generator i, and $P_{di,\max}$ is the maximum active power output of generator i. Furthermore, the spinning reserve demand considered for safe and reliable operation of the diesel power generators are described as follows:

$$\sum_{i=1}^{N_{DG}} SP_{di} \geqslant SP_R \tag{12}$$

$$SP_{di} = P_{di,\max} - P_{di} \tag{13}$$

where SP_{di} is the spinning reserve contribution of the diesel generator i and SP_R is the spinning reserve requirement of the system.

4.1.5. Battery agent (BA)

The battery storage system is represented by an agent. This agent will monitor the charging, discharging and SOC of the battery storage systems. This agent will be activated when the renewable energy systems cannot provide enough supply to the load demand. In this microgrid, the battery agent will control the charging and discharging of the batteries.

The SOC of the battery is limited between a minimum of 20% to a maximum of 100% of its Ampere-hour capacity. This is to prevent undercharging and overcharging of the battery bank, thus prolonging its life. The batteries' charging constraints are expressed as follows:

$$\mathrm{SOC}_{\min} \leqslant \mathrm{SOC}(t) \leqslant \mathrm{SOC}_{\max} \tag{14}$$

Similarly, the battery agent will also control the maximum permissible charge and discharge current of the batteries which is limited at 10% of the battery capacity. The battery charging and discharging constraints are expressed as follows:

$$P_c, P_{dc} \leqslant \frac{0.1 V_{bat} Q_{bat}}{\Delta t} \tag{15}$$

where P_c is the charge power (kW) and P_{dc} is discharge power (kW), whereas V_{bat} is the voltage at the battery AC link and Δt is the time step (seconds).

4.1.6. Grid agent (GA)

The electricity distribution network of the microgrid is also represented by an agent. This agent will monitor both the transmission and distribution parameters. Thus it will detect any faults occurring on the grid and respond accordingly by sending information to the agents. In order to prevent overloading, the grid's transmission is constraint considered in order to ensure the lines will not exceed its loading limit. The loading limit is represented as follows:

$$\max[LF_{bi}, LF_{bj}] \leqslant LF_{k,\max} \tag{16}$$

where LF_{bi}, and LF_{bj} are real power flow from bus i to bus and bus j to bus i, respectively, whereas, $LF_{k,\max}$ is the kth branch maximum loading limit.

4.1.7. Load agent (LA)

This entire microgrid system's load is represented by one load agent. This load agent will monitor whether the load demand for each time step is satisfied accordingly by the power generation systems. The load agent also will control the secondary load bank when there is a needs to dump the surplus power generated by the RE system when the battery system is fully charged.

4.2. MAS architecture for EMS

4.2.1. Mode classification

The behavior of each component in the microgrid has been classified according to several modes of operation: The modes are expressed as follows:

$$M = \{M_1, M_2, M_3, M_4\} \tag{17}$$

where M_1 is defined as active, M_2 is hot standby, M_3 is cold standby and M_4 is inactive. The active mode indicates that the microgrid component is currently supplying energy to the grid. Meanwhile, hot standby mode means the component is capable of providing energy, but it is not selected by the EMS. The component incapable of providing power due to environmental limitations is designated by the cold standby mode, whereas, inactive mode shows that the component is in service for repair or maintenance and, therefore cannot deliver power to the grid. The EMS control task is a combination of continuous control and discrete decision making. Both processes have several differences in handling the mode changes in the system.

As shown by the agent architecture in Fig. 4, the agent's process can be divided into two parts which are the decision-making in the cooperative layer and continuous control in the planning layer. The decision process in the cooperative layer is shown in Fig. 5, where the mode varied according to the environmental conditions. If the environment satisfies the running conditions, the mode will be changed to M_2, otherwise the agent's will be assigned with M_3. If the agent's mode stays at M_3 for more than the threshold time, T_{M3}, it will be assigned with M_4. Meanwhile, as for the continuous control process in the planning layer, if the selected power generator is at M_2 in the decision making process, the mode will be changed to M_1. If the component is not selected as the power supplier, it will remain as the same mode as in the decision making process. The flow of the process in the continuous control block in the agent architecture is shown in Fig. 6. The implemented mode selector in the Simulink Stateflow is shown in Fig. 7.

As illustrated in Fig. 4 and Table 1, there are three layers in the agent architecture where the information moved from bottom to top and the control instruction flows from top to bottom. The overall agent process in the three layers can be summarized as follows: First, the agent will continuously monitor its mode. As soon as the agent detect its mode changed to either M_3 or M_4, it will compare with the previous mode and decides if reorganization order is needed or to response directly. Else, if the reorganization order from EMS is received, it will send parameters such as current mode and expected output capacity from the agent's layer (local planning layer) to the upper layer (cooperative layer). Then, it will send the parameters to other agents for cooperation. Once it receives the global decisions from other agents, it will make decision, switch its mode and step back into the continuous control cycle. The flow of agent processes in decision making is shown in Fig. 8.

4.2.2. Primary facilitator

The facilitator approach was initially proposed in [37] where multiple related agents were grouped and the facilitators acted as an interface for information sharing between the agents. In this work, the facilitator approach has been implemented for the microgrid EMS structure. Facilitators are introduced into the power generators and battery agents. The main aim of facilitator introduction is to decrease the communication burden among agents in the system, providing a reliable communication network and coordinating the control of multi-agent activities. The MAS control structure for the EMS is shown in Fig. 9.

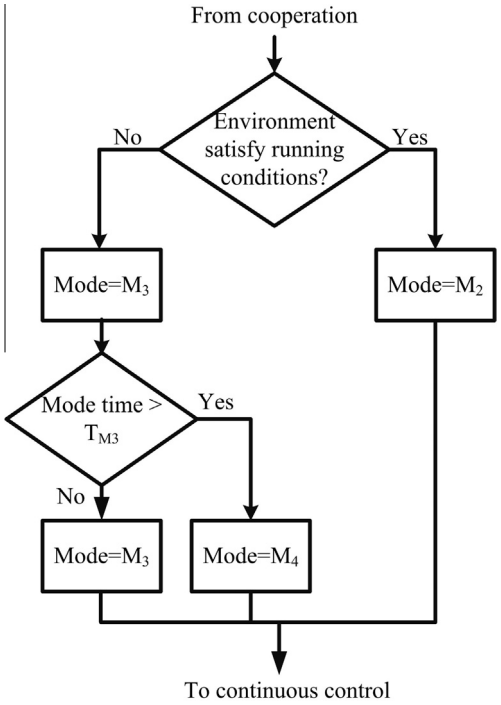

Fig. 5. Decision making process.

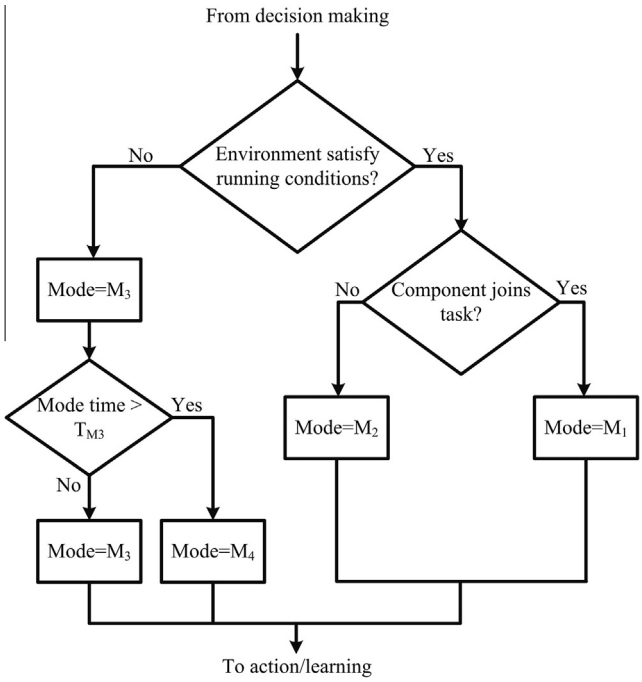

Fig. 6. Continuous control process.

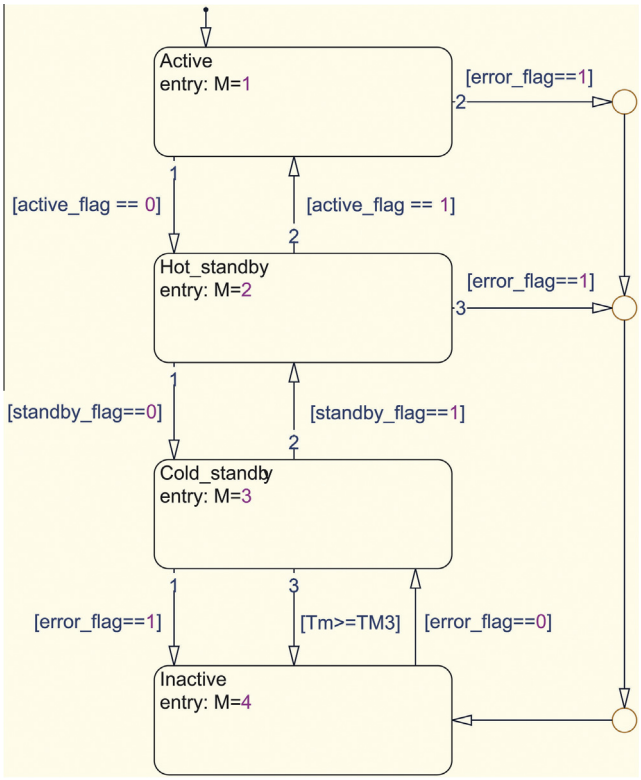

Fig. 7. Simulink Stateflow chart for mode selection.

Although this EMS strategy is based on individual agent characteristics and behavior, facilitators are present in order to perform global optimization for the whole system. Therefore, during the optimization process, each agent will adjust their decisions adaptively based on their structure and behavior, but facilitators will give instruction to agents and make the final decision in order to avoid conflict between agents. The facilitator that makes the decision at the specific time is called the primary facilitator and will make decisions based on the global optimization function. Each facilitator in the system is capable of being promoted to primary facilitator. However, at any specific time, only one primary facilitator will be chosen.

The facilitators are structured based on a virtual token ring network where the facilitator who holds the token is the primary facilitator and in charge of making decisions. The flow of the virtual token and facilitator process are illustrated in Fig. 10.

4.2.3. Structure

The MAS in this microgrid system has three primary layers that include individual, colony and system layers with optimization executed from bottom to top, whereas the decision process will be carried out from top to bottom. Fig. 11 shows the proposed MAS structure.

4.3. Global optimization

The energy management system must be able to optimize the microgrid and maximize the system's benefits. In this paper, the optimization primary goal is to minimize the usage of diesel generators on a daily basis (24 h), thus reducing the energy cost and emissions. Therefore, an objective function is formulated for the energy management system.

The objective function goal is to minimize the daily total generation cost. The function is expressed as:

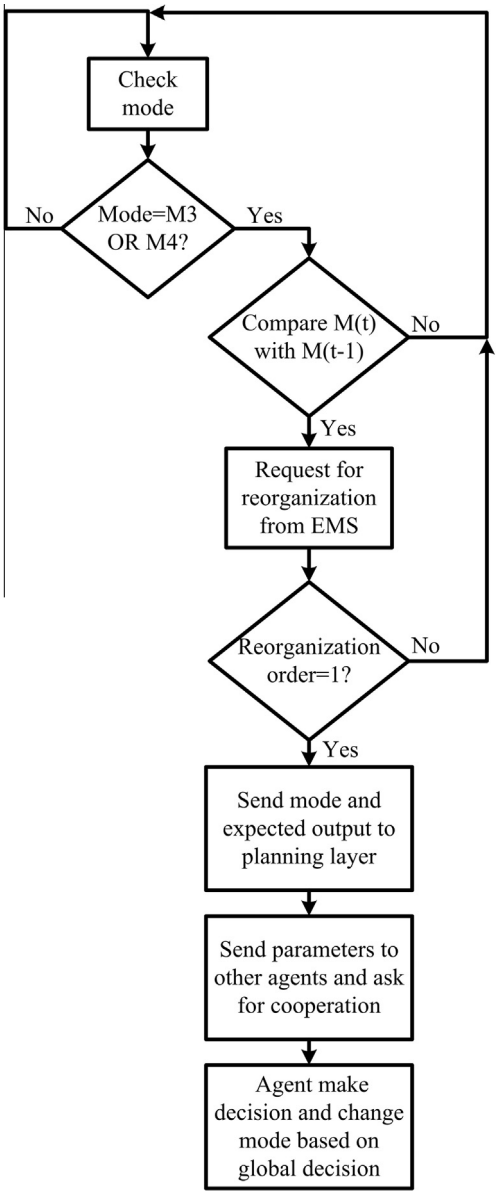

Fig. 8. Simplified agent processes.

$$\text{minimize } f = \sum_{t=1}^{T}\sum_{i=1}^{N_G} x_{it} P_{it} c_{it} \tag{18}$$

$$\text{subject to } \sum_{t=1}^{T}\sum_{i=1}^{N_G} (x_{it} P_{it} - P_{load,it} - P_{losses,it}) = 0 \tag{19}$$

where c_{it} is the energy cost, P_{it} is the power output of each type of power supply, $P_{load,it}$ is the load demand, $P_{losses,it}$ is the total power losses, t is the index for time slot, i is the index for type of energy source, T is the total intervals in one day which is equivalent to 24, and N_G is the total sum of energy sources.

The x_{it} value is computed by each individual agent. It represents the agent intention to provide energy supply during this situation where its values implies specific meaning of the particular agent intention as follows:

$$x_{it} = \begin{cases} 0, & \text{Agent has no intention to provide power } (M_3 \text{ or } M_4) \\ 1, & \text{Agent has intention to provide power } (M_2) \end{cases} \tag{20}$$

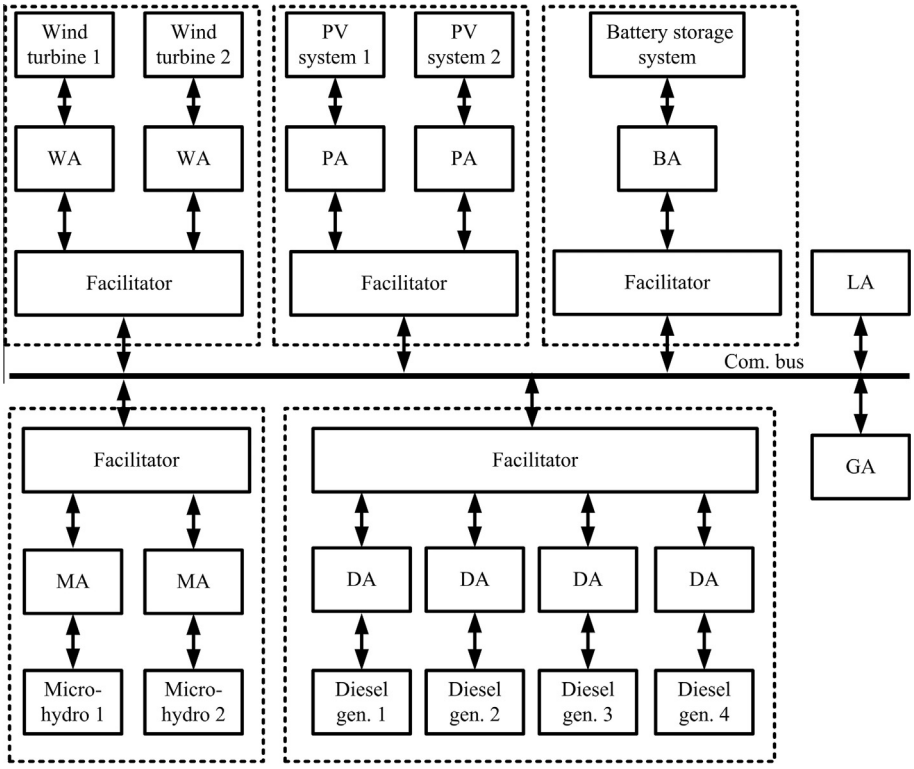

Fig. 9. MAS control structure for DGS.

The new formulated global objective function has several major distinctions compared to previous models of energy management systems [2,38,39]. Firstly, it does not have a fixed time step. The optimization function will be executed once excited by the grid based on the changes in renewable resources, load demand, output power, and other grid parameters. Next, the energy sources mode, x_{it} is incorporated into the optimization function. Hence, each component in the microgrid will compute and make decisions based on its intention and competence. Therefore, not only the global optimization is crucial and needs to be attained, but the agent's decision will also be incorporated for overall decision making. This MAS based EMS optimization function also has minimal constraints since each microgrid component will satisfy its own constraints realized by each component's agent. Thus, this will reduce the communication and computational burden of the entire system.

5. Game theory for multi-agent coordination

A new energy balance strategy for multi-agent coordination based on non-cooperative game theory was developed to optimize the energy dispatch and costs in the microgrid based on the global objective function, as in Section 4.3. In this study, game theory was used as a strategic analysis for handling competitive situations where the result of one agent's choice of action was influenced by the action of other agents. The game theory was specifically designed to handle the resource allocation problem of the economic dispatch in the DGS that consists of multiple renewable energy resources and a battery storage system. Compared to centralized EMS, the advantages of using the game-theory approach for multi-agent based distributed EMS is that little computation is needed from each individual agent to achieve optimal dispatch. Hence, this will reduce the computation load on a single controller resulting in faster decision and controls.

5.1. Strategic games

A normal form game also known as strategic game comprises of players, strategies or action profiles for each player and utility function or payoff for each strategy combination. The game structure is described as follows [17]:

$$G = \langle P, S, F \rangle \tag{21}$$

where finite set of n players indexed by i described as follows:

$$P = \{P_i, P_{i+1}, \ldots, n\} \tag{22}$$

The strategy set is an n-tuple of pure strategy profiles, available for each player i as follows:

$$S = \{S_i, S_{i+1}, \ldots, S_n\} \tag{23}$$

The payoff function is denoted by:

$$F = \{F_i, F_{i+1}, \ldots, n\} \tag{24}$$

where F_i: $S \mapsto \mathbb{R}$ is a real value payoff for player i.

In the prisoner's dilemma, each player (agent) will try to maximize his own payoff, with no interest in opposing player payoff [17]. In this study, this type of game was implemented because of its simplicity therefore reducing the computational complexity while still optimizing the coordination between agents.

The general form of prisoner's dilemma payoff matrix is shown in Fig. 12.

Where the prisoner's dilemma is any strategic game that each player can choose to either Cooperate (C) or Defect (D).

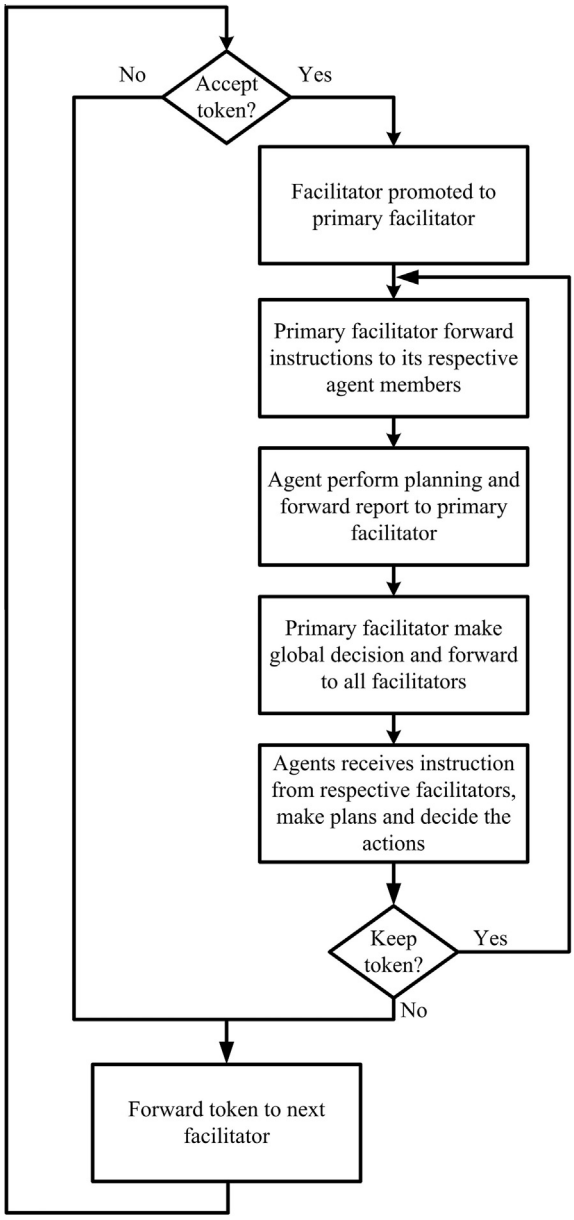

Fig. 10. Facilitator process and virtual token flow.

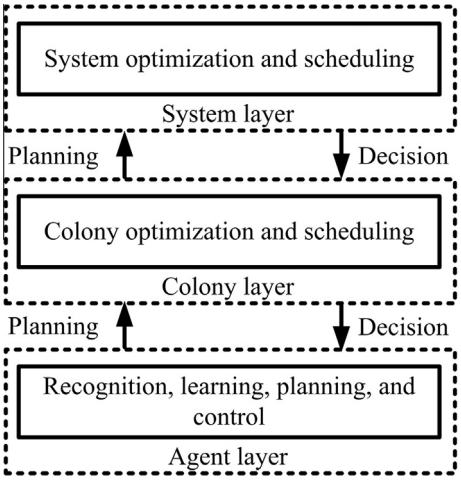

Fig. 11. Structure of MAS for the EMS.

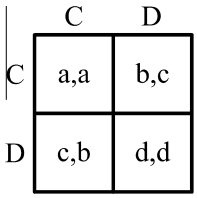

Fig. 12. Prisoner's Dilemma payoff matrix.

5.2. Game elements

5.2.1. Players

There are five players in the game: PV, wind, micro-hydropower, battery storage, and diesel generator systems denoted by PV, W, MH, BS and DG respectively.

5.2.2. Strategy

In this non-cooperative game, the agent will communicate with other agents and will play games based on the best strategy that will maximize their power production while having minimal operating cost. When playing the game, each agent will try to choose the best strategy to play based on both their own power production capability and the opponent's power production capability. Each agent will play games with other agents only when requested by the primary facilitator to reduce the computational and communication burden of the system. In this paper, the agent will play games and make the decision to either join the mixed power generation or not, based on their load demand and their power output. The strategies for each player are as follows:

$$S_i = \{Dispatch, Idle\} \tag{25}$$

where S_i represents the ith player strategies.

5.2.3. Payoff functions

Several factors have been considered for determining the payoff of each player in the game such as the power output and load demand. The payoff matrix for each player has been predetermined which is unique and distinct according to the type of energy sources. The payoff values are based on the global objective function where it is normalized to value ranges from 0 to 1. When instructed by the primary facilitator, an agent will play a two player game with each generator agent. Since the payoffs are based on the global objective function, the input parameters for the game are the power outputs, generation cost, and agent modes. The output results of each game will be returned to the primary facilitator. The example of the game performed by an agent is illustrated in Fig. 13. Later, based on the game results, the primary facilitator will make a decision and send it to other facilitators. The example of a payoff matrix between two players is as follows:

		Wind system	
		Dispatch	Idle
A = PV system	Dispatch	0.8, 0.8	1,0
	Idle	0,1	0.2, 0.2

The dilemma for each RE agent is that they could achieve better results by dispatching most of the time. Hence, based on the global objective function, the dominant strategy for RE agent is to cooperate. However, for battery and diesel generator agent, the dispatch strategies are chosen based on the most optimal and economical solution at that particular time.

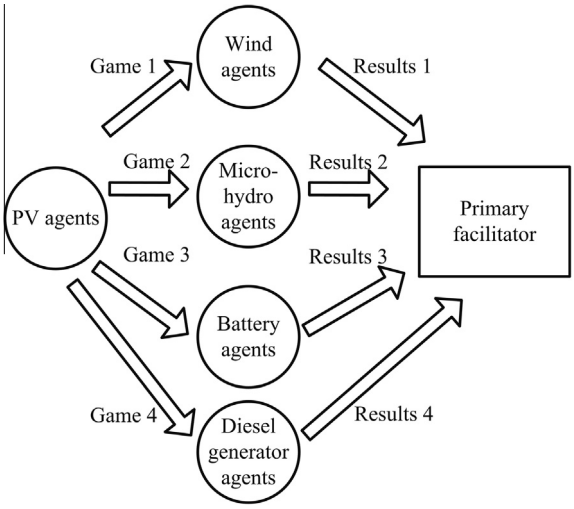

Fig. 13. Sample game flow performed by one agent.

5.3. Strategies

The strategy of player i is called dominance when it generates greater payoff than the other strategy regardless of how the other player (denoted as $-i$) plays as shown below [17]:

$$F_1(s_i, s_{-i}) \geqslant F_1(s_i', s_{-i}) \tag{26}$$

s_i and s_i' are the two strategies of player i, and the other player's set of strategy profiles is denoted by S_{-i} where $s_{-i} \in S_{-i}$.

The stable strategy profile is the called Nash equilibrium where no player/agent wishes to change his strategy even if he knew the strategies of another player/agent [17]. There are two types of Nash equilibrium: strict and weak.

The set of strategies $S = (s_i, \ldots, s_n)$ is a strict Nash equilibrium for agent i if:

$$\forall i, s_i \in S_i : F_i(s_i, s_{-i}) > F(s_i', s_{-i}), \tag{27}$$

where if the inequality above is denoted by $\geqslant$ instead of >, then it is classified as a weak Nash equilibrium.

In this paper, the iterative search procedure, as in [40], was used for finding the Nash equilibriums of the game between agents, but it is not covered in this paper. The flowchart for finding the Nash equilibrium is shown in Fig. 14.

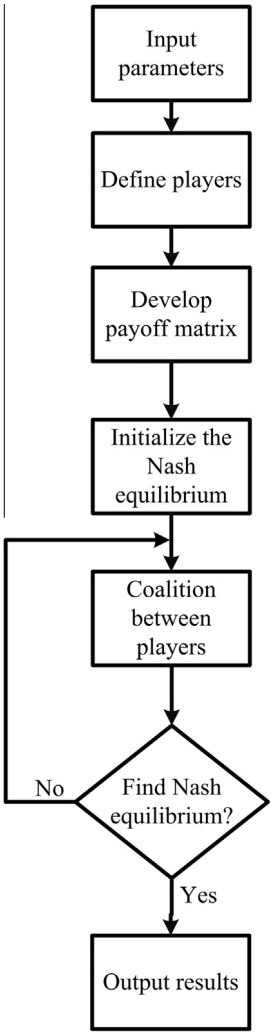

Fig. 14. Basic flow chart for multi-agent coordination based on game theory.

6. Simulation and results

6.1. Case study

The simulation was carried out considering the current energy situation on Tioman Island as a case study. The electricity on the island is distributed through 11 kV distribution networks. A diesel plant is the main 24-h power supply for the island, whereas the distributed diesel generators act as a power backup during peak load demand when the main diesel generators have output constraints.

The diesel plant comprised of one diesel generator with rated capacity of 2.5 MW and three diesel generators with rated capacity of 500 kW. The 2.5 MW diesel generator operates as a base station, with its output complemented by the three 500 kW diesel sets. The EMS has been modeled based on the island's currently installed power generation systems with additional distributed micro-hydropower, PV, and wind power generation systems as shown in Fig. 2.

The modeled loads approximately represent the type of loads available on the resort island comprised of resort hotels and a community of hundreds of village households. The load was simulated according to the real variation of daily load profile on the island. The island community has a base load of 1.5 MW during monsoon season and 2 MW during non-monsoon season. In this paper, the simulation will be carried out considering only non-monsoon season daily load profiles as shown in Fig. 15.

The average minimum load demand for the non-monsoon season is 948.05 kW and 668.02 kW during the monsoon season. The actual meteorological data for Tioman Island was obtained from MMD (Malaysian Meteorological Department) and also the NASA POWER (NASA Prediction of Worldwide Energy Resource) database. The solar radiation, wind speed and streamflow data for a typical day in non-monsoon season used in the simulation are shown in Fig. 16. Since, there were no hourly streamflow data available, the streamflow data was synthesized based on the daily average streamflow and hourly wind speed. The main parameters for the renewable energy generation systems are shown in Table 2. The levelized cost of energy (LCOE) for the entire system from previous study has been used to approximately represent the energy cost for each power generation [41]. The total energy cost of the battery storage system also includes the battery wear cost in addition to the average energy cost. The costs used in this scenario are presented in Table 3.

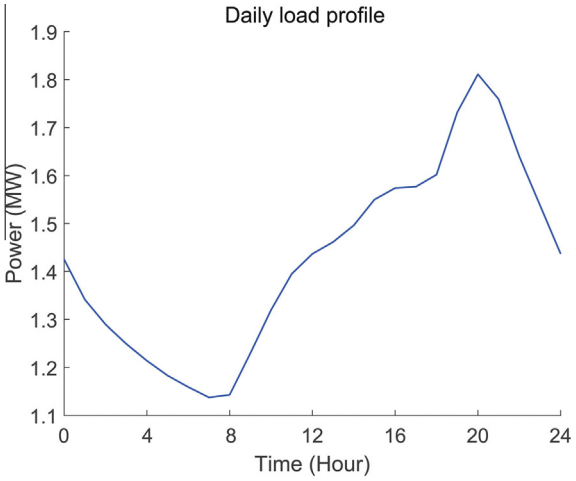

Fig. 15. Daily average load profile during non-monsoon season.

6.2. Simulation

The simulation in this study lasted for 24 h. As shown in Fig. 16, the solar radiation profile followed a typical pattern where the highest intensity occurred during midday. Meanwhile, the wind speed and streamflow varied significantly throughout the day with several peaks and lows. As for the load profile, the maximum load demand took place at 20.00, whereas the minimum load demand occurred at 07.00. Since the case study was based on a resort island, it had a distinct load profile due to tourist activities during the day. The energy demand profile started low during the day and rose to a peak in the evening, and later gradually dropped in the night.

In order to evaluate the performance of the new distributed control architecture, several scenarios such as resource fluctuations and load demand variations, that will disturb the grid frequency during the day, were simulated.

6.2.1. Scenario 1

In this scenario, there were no disturbances simulated. The system ran based on the load profiles and renewable resources input parameters as shown in Figs. 15 and 16, respectively. This scenario was simulated in order to determine the system performance during normal operation where no disturbances occurred. The power output of the system from several resources during normal operation throughout the day is shown in Fig. 17. Meanwhile, the grid frequency is shown in Fig. 18.

In this scenario, only 2.5 MW diesel set was used where the other diesel generators were turned off during the day. The agents for the generation systems were in 'active' mode throughout the day except for the PV system and the supplementary diesel generators. The PV system agents were in 'active' mode from 07:00 to 19:00 and stayed 'inactive' for the rest of the day. Meanwhile, the 500 kW diesel generators modes were 'inactive' for the whole day. On the other hand, the battery agent was in 'cold standby' when it was not discharged and changed to 'active' mode when it started to supply power to the grid.

The RE system significantly reduced the diesel power consumption from 11:00 to 13:00 due to high availability of all RE resources. It can be seen that the PV and micro-hydropower systems were able to provide power throughout the day, whereas the PV system only provided power to the system from 07:00 to 19:00.

During nighttime, the battery agent discharged the battery in order to reduce diesel fuel consumption which is illustrated by the battery SOC as shown in Fig. 19. The battery initially had 80% of its SOC which later dropped to 20% at the end of the day. In this scenario, there was no excess energy generated from the RE system. Therefore the battery was not charged throughout the day. There were several events disturbed the grid frequency throughout the day such as charging and discharging of the battery bank. In this scenario, the frequency was recovered to 50 Hz within an average of 3.2 s.

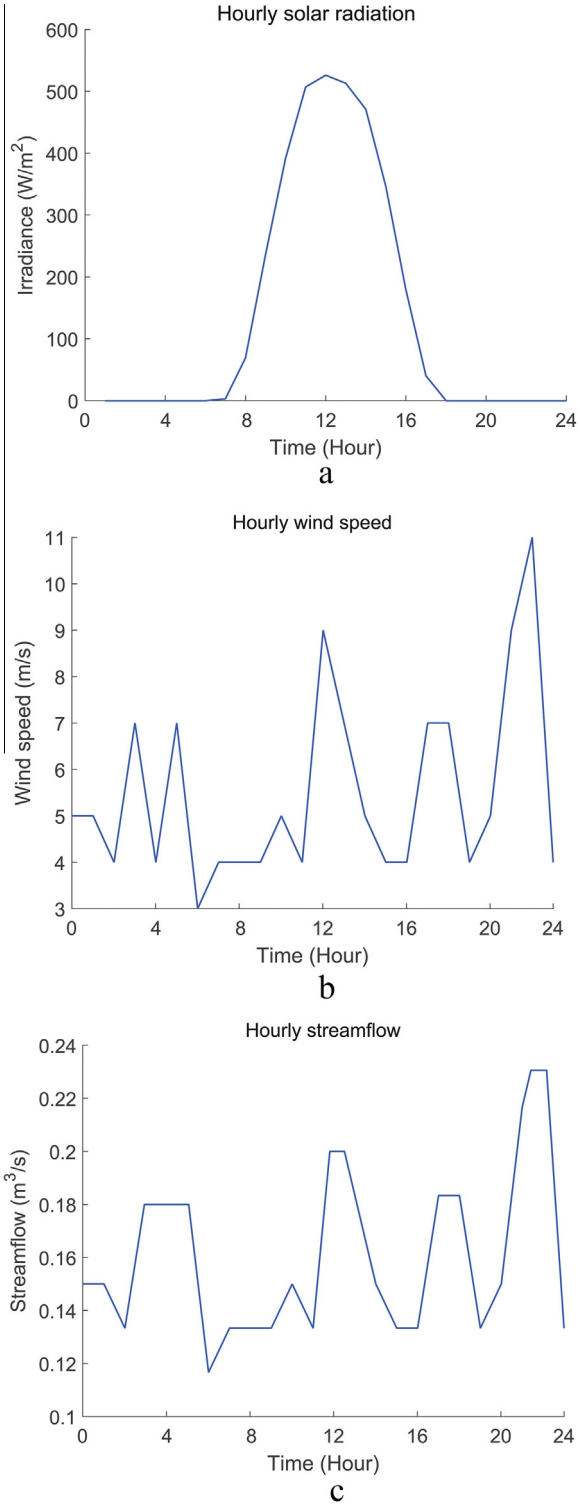

Fig. 16. Renewable resource data for a day in non-monsoon season (a) solar radiation (W/m^2), (b) wind speed (m/s) and (c) streamflow (m^3/s).

Table 2
Renewable energy generation and battery storage parameters.

Description	Specifications
1. PV system	
Type	Monocrystalline
Efficiency (%)	10
Area (m^2)	5000
2. Wind system	
Nominal power output (kW)	250
Cut in wind speed (m/s)	2.5
Rated wind speed (m/s)	7.5
Cut out wind speed (m/s)	11
3. Hydropower system	
Nominal power output (kW)	250
Rated streamflow (m^3/s)	0.25
Efficiency (%)	70
Head height (m)	141
4. Battery storage system	
Nominal voltage (V)	400
Battery capacity (A h)	10,800
Nominal discharge current (A)	700
Efficiency (%)	90

Table 3
Energy costs.

Energy sources	Price ($/kW h)
PV	0.070
Wind	0.078
Hydro	0.045
Diesel	0.157
Battery	0.056

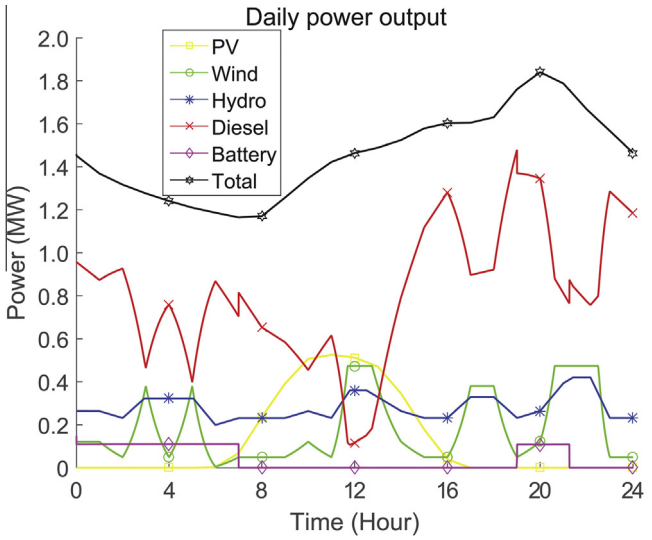

Fig. 17. Daily power output for scenario 1.

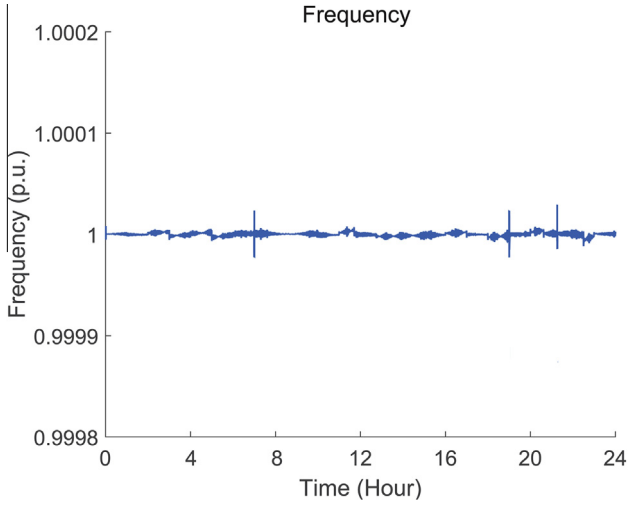

Fig. 18. Grid frequency for scenario 1.

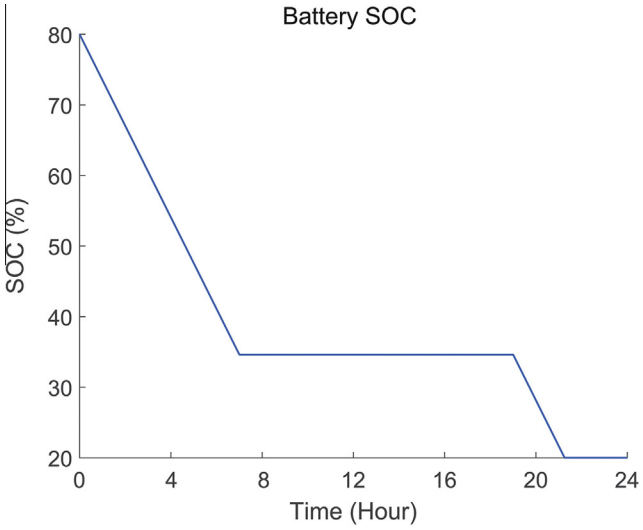

Fig. 19. Battery SOC for scenario 1.

Table 4
Simulated events/disturbances for scenario 2.

Time (s)	Event/disturbances
10:30–11:00	Partial shading compromising the power generation of the PV systems
12:00–13:00	RE power generation exceeds the load demand
22:00–23:00	Wind speed surpasses the cut-out speed of wind turbines

6.2.2. Scenario 2

This scenario, there were several events or disturbances simulated as listed in Table 4. All the events were simulated in order to assess the microgrid capability of handling variations in renewable resources. In order to simulate RE generation exceeding the load demand, streamflow data were adjusted to simulate the possibility of higher micro-hydropower generation at noon, as illustrated in Fig. 20. The power output of the system throughout the 24 h simulation time is shown in Fig. 21.

Similar to scenario 1, only the 2.5 MW diesel set was running throughout the day. The agent's modes throughout the 24 h in this scenario were also similar to those in scenario 1, except for the wind system. The partial shading that occurred from 10:30 to 11:00 affected the power generated by the PV system, causing the PV output to suddenly drop from 561 kW to 359 kW. The PV output rose to 527 kW after the partial shading occurred. The partial shading also caused the microgrid frequency to deviate for a moment as shown in Fig. 22. In this scenario, the frequency recovered to 50 Hz within an average of 4.02 s.

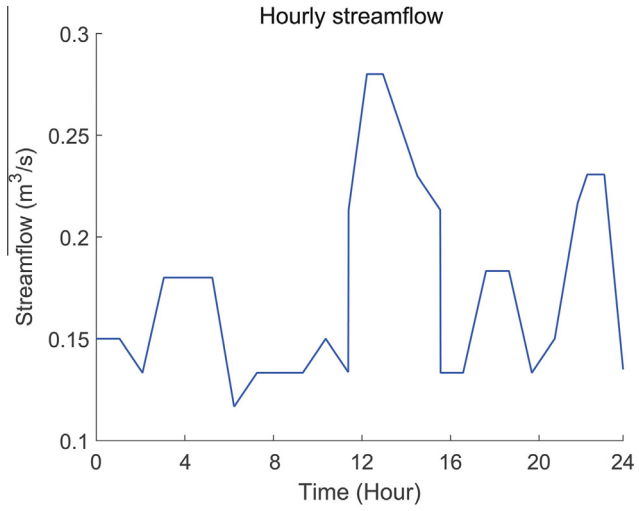

Fig. 20. Streamflow data for scenario 2.

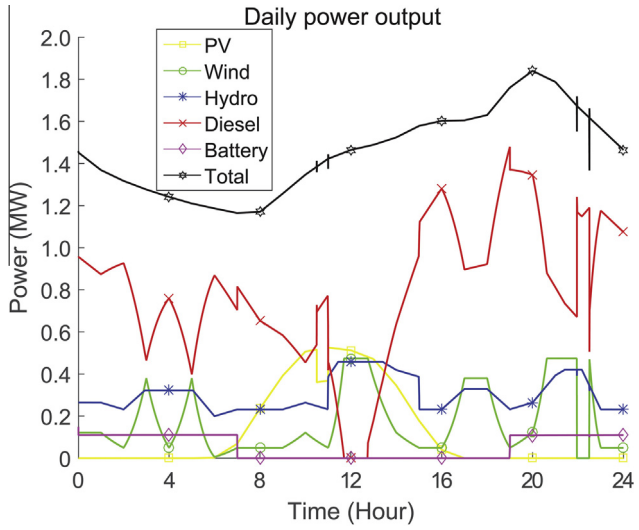

Fig. 21. Daily power output for scenario 2.

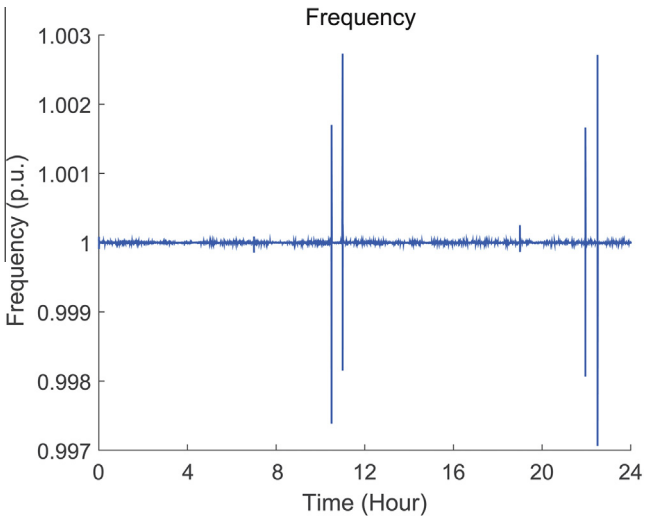

Fig. 22. Grid frequency for scenario 2.

From 12:00 to 13:00, it can be seen that the RE generation exceeded the load demand, hence the diesel generator turned off. The total average RE generation during the period was 1.60 MW whereas the average load demand was 1.46 MW. Thus the surplus power, an average of 140 kW was used to charge the battery storage system for a period of one hour as shown by the battery SOC in Fig. 23.

The wind speed surpassed the cut-out speed of the wind turbines from 22:00 to 23:00 causing the wind systems to trip from the grid. The wind system turned on when the wind speed returned to its rated value. The wind system agents were in 'active' mode throughout the day but went to 'inactive' when it was tripped from the grid and became 'active' again when it started to supply power to the grid. It can be seen in Fig. 22 that the tripping of the wind system caused the microgrid frequency to deviate.

6.2.3. Scenario 3

In this third scenario, the microgrid performance was assessed considering the load side disturbance as listed in Table 5. A 0.2 MW asynchronous machine model was used in order to simulate the commercial load effect on the grid and was turned on at 20:00.

A 24 h load profile with 2.8 MW peak was used for simulating the microgrid behavior when one diesel generator was not capable of catering to the load demand. The load profile for this scenario is shown in Fig. 24.

It can be seen from the power output results in Fig. 25 that the grid frequency deviated as soon as the commercial load was turned on. For this scenario, diesel generator 2 was set to turn on when the total load demand went beyond 2.5 MW, exceeding diesel generator 1's maximal capacity.

It can be seen on the diesel generators power output as shown in Fig. 26, that the 500 kW diesel generator was turned on when the load demand exceeded 2.5 MW. The RES able to provide additional power to meet the load demand. However, when the load

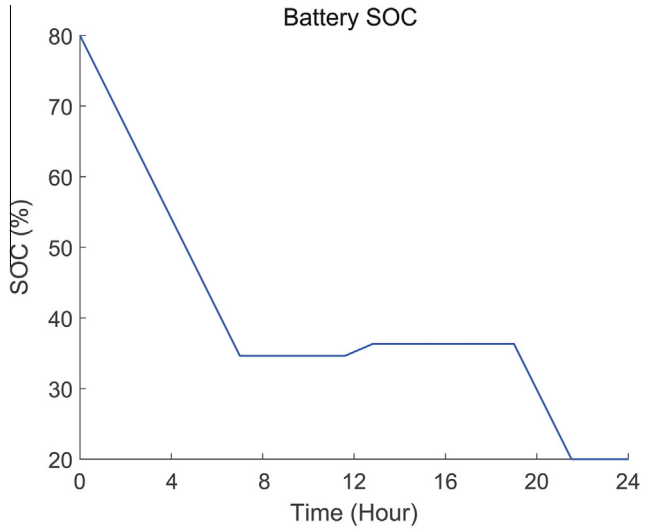

Fig. 23. Battery SOC for scenario 2.

Table 5
Simulated events/disturbances for scenario 3.

Time (s)	Event/ disturbances
15:00	The total load demand goes beyond 1.8 MW
20:00	Asynchronous machine started simulating the effect of commercial load

Fig. 24. Load demand for scenario 3.

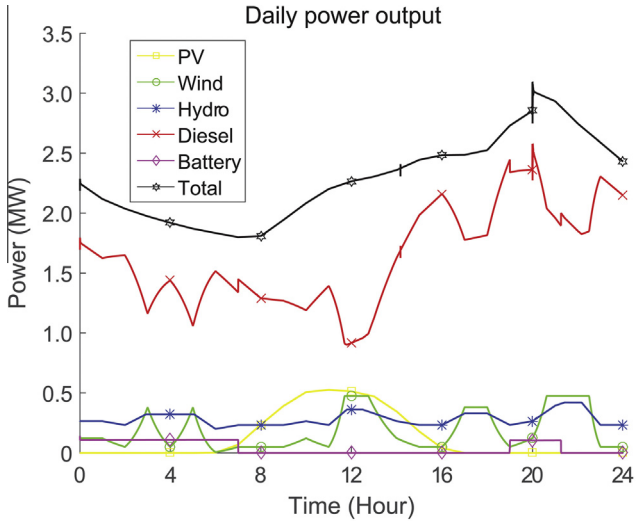

Fig. 25. Daily power output for scenario 3.

reached 2.5 MW, diesel generator 2 was turned on in order to ensure the power generation was able to meet the load demand in case there were not enough RE resources available. As shown in Fig. 27, it can be seen that both of the disturbances affected the grid frequency and the EMS managed to return the frequency back to 50 Hz within an average of 3.66 s.

6.2.4. Scenario 4

In scenario 1 to scenario 3, the system simulation runs for 24 h only. To have a better insight of the control performance, longer runs need to be simulated, especially considering the battery SOC is less than 80% or depleted after the 24 h run. It is also necessary to simulate the microgrid performance of another day, where the initial SOC of the battery is less than 80%. Hence, in scenario 4, the initial battery SOC was set to 20% and the system's performance in response to this situation was assessed. The input load profile used, as in Fig. 15, and the renewable resources used such as solar radiation and wind speed used, are shown in Fig. 16. Meanwhile, the streamflow input is as in Fig. 20.

This scenario only intended to simulate the microgrid performance when the battery has low SOC at the beginning of the day. Hence, there were no disturbances simulated. The simulation results show that only the 2.5 MW diesel generator was running all day where the supplementary diesel generators were turned off during the day. Except for the PV system and the supplementary diesel generators, other generation systems agents were in 'active' mode all day. The system's power output from mixed generations throughput the day is shown in Fig. 28.

The PV system agents were in 'active' mode during the availability of solar radiation which is from 07:00 to 19:00 and stayed 'inactive' for the rest of the day when there was no solar radiation, whereas the 500 kW supplementary diesel generators modes were 'inactive' throughout the day. In contrast, the battery agent was in 'active' mode when it was supplying power to the grid and in 'hot standby' when it had SOC higher than 20%, but was not discharged. The battery was in 'cold standby' when it has SOC lower than 20% during the day.

In this paper, the load following dispatch strategy was used. Therefore, only renewable power sources will charge the battery. The diesel generators will produce sufficient power to serve the load only, and will not charge the battery bank.

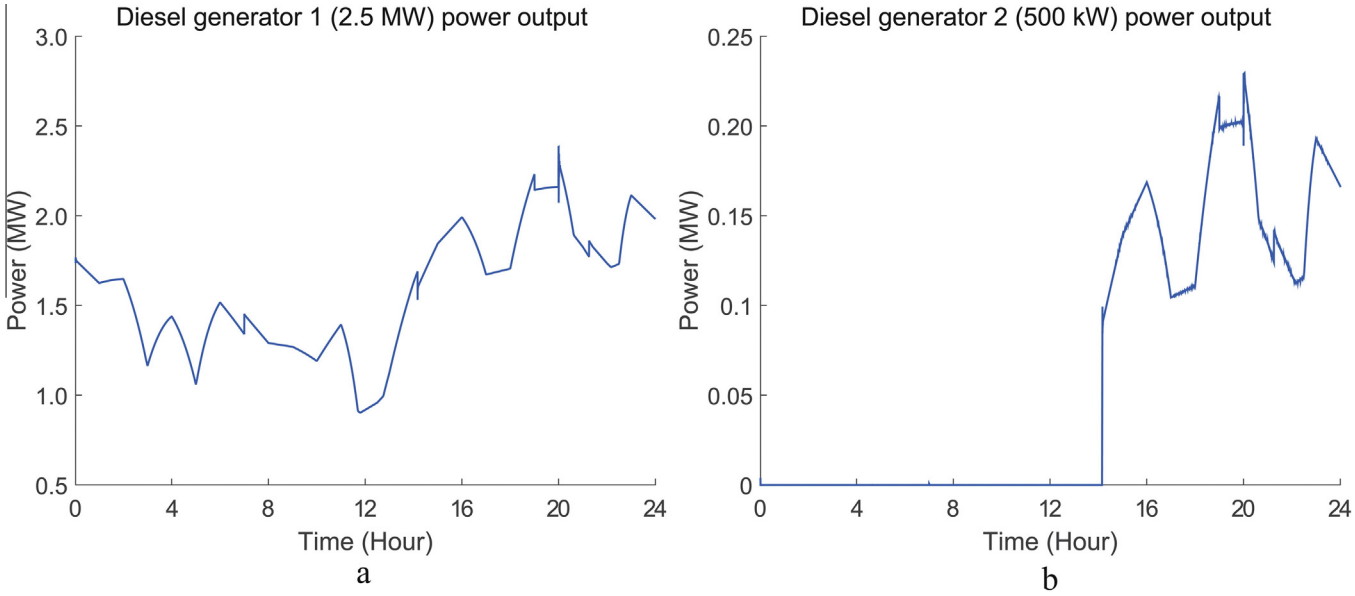

Fig. 26. Diesel generators power output for scenario 3 (a) diesel generator 1 and (b) diesel generator 2.

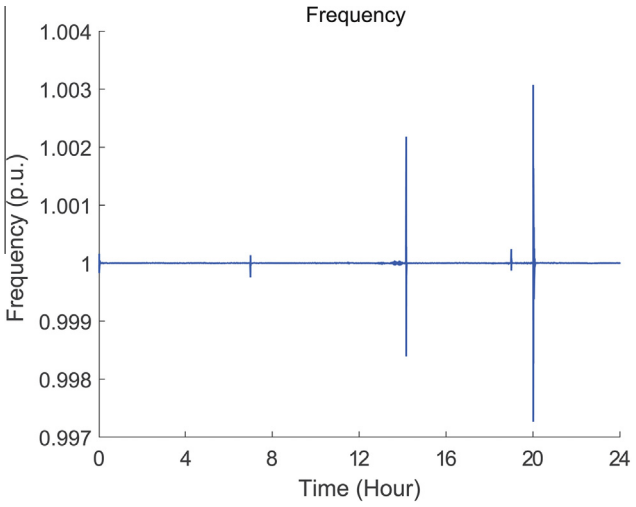

Fig. 27. Grid frequency for scenario 3.

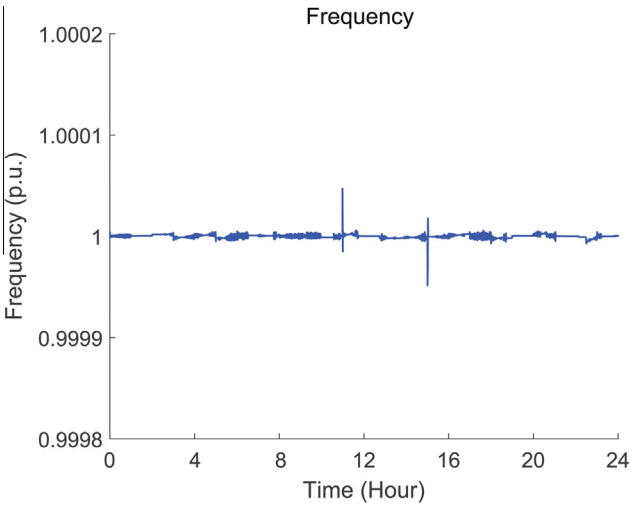

Fig. 30. Grid frequency for scenario 4.

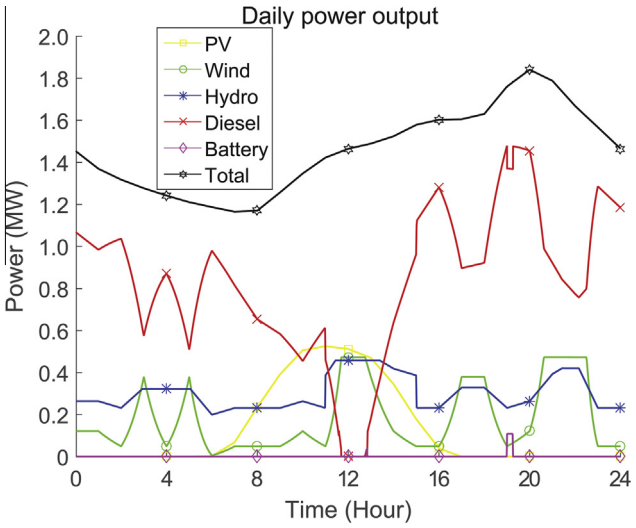

Fig. 28. Daily power output for scenario 4.

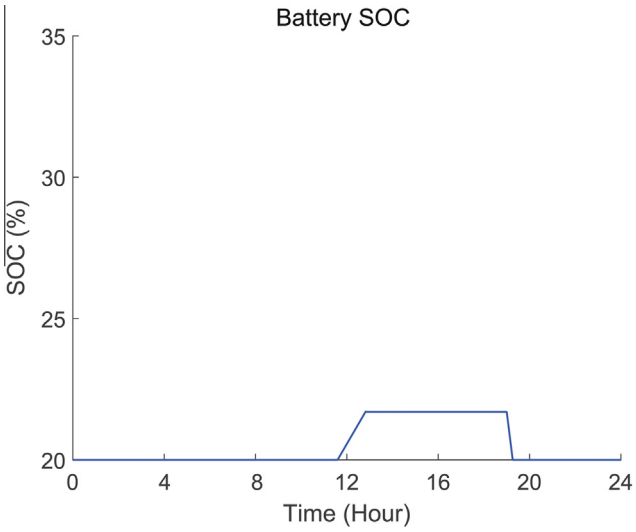

Fig. 29. Battery SOC for scenario 4.

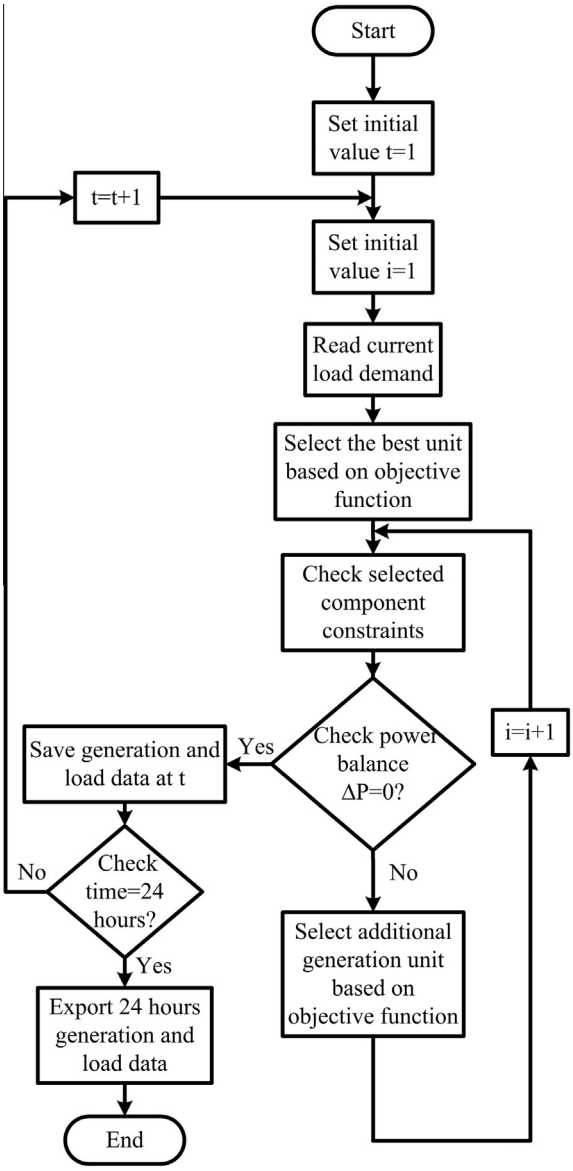

Fig. 31. Basic flowchart for the centralized EMS strategy.

In the simulation results, high micro-hydropower generation at noon causes the diesel generation system to be turned off from 12:00 to 13:00, and the load demand has been supplied by the RE systems only. During this period, the excess power from the RE system has been used to charge the battery. As shown in Fig. 29, the battery initially had 20% of its SOC which later charged up to 23% by the excess power generated by the RE system. Later, the battery agent discharged the battery to mitigate the diesel fuel consumption at 19:00. The charging and discharging of the battery bank causes the microgrid frequency to deviate as shown in Fig. 30. However, the frequency spikes managed to be kept within limits and recovered to 50 Hz within 3.57 s. In this paper, the simulation performed for assessing the performance of multi-agent in handling disturbances occurred in the microgrid. Although, the initial SOC of the battery bank in this scenario was at 20%, it does not create problems to the grid. It will only affect the total efficiency of the microgrid, due to higher usage of diesel generator throughout the day.

Table 6
Performance results of multi-agent EMS and centralized EMS.

	Multi-agent based EMS				Centralized EMS			
	S1	S2	S3	S4	S1	S2	S3	S4
η_{sys}	0.771	0.753	0.684	0.798	0.639	0.603	0.54	0.696
η_{pv}	0.853	0.772	0.612	0.887	0.677	0.621	0.517	0.784
η_{wind}	0.885	0.813	0.673	0.911	0.653	0.643	0.533	0.827
η_{hydro}	0.856	0.828	0.654	0.897	0.687	0.668	0.526	0.812
P_{loss} (%)	1.211	2.039	3.634	1.332	2.541	4.037	7.636	2.127

6.3. Microgrid performance evaluations

The microgrid efficiency has been assessed based on [42] and has been modified and simplified accordingly in order to suit this study. The whole system efficiency was defined based on the ratio between the total load demand and both total renewable energy and fossil energy generations. The battery storage was not included in the efficiency analysis due to its behavior, acting as either power supply or load during the day. The overall system's efficiency is expressed as follows:

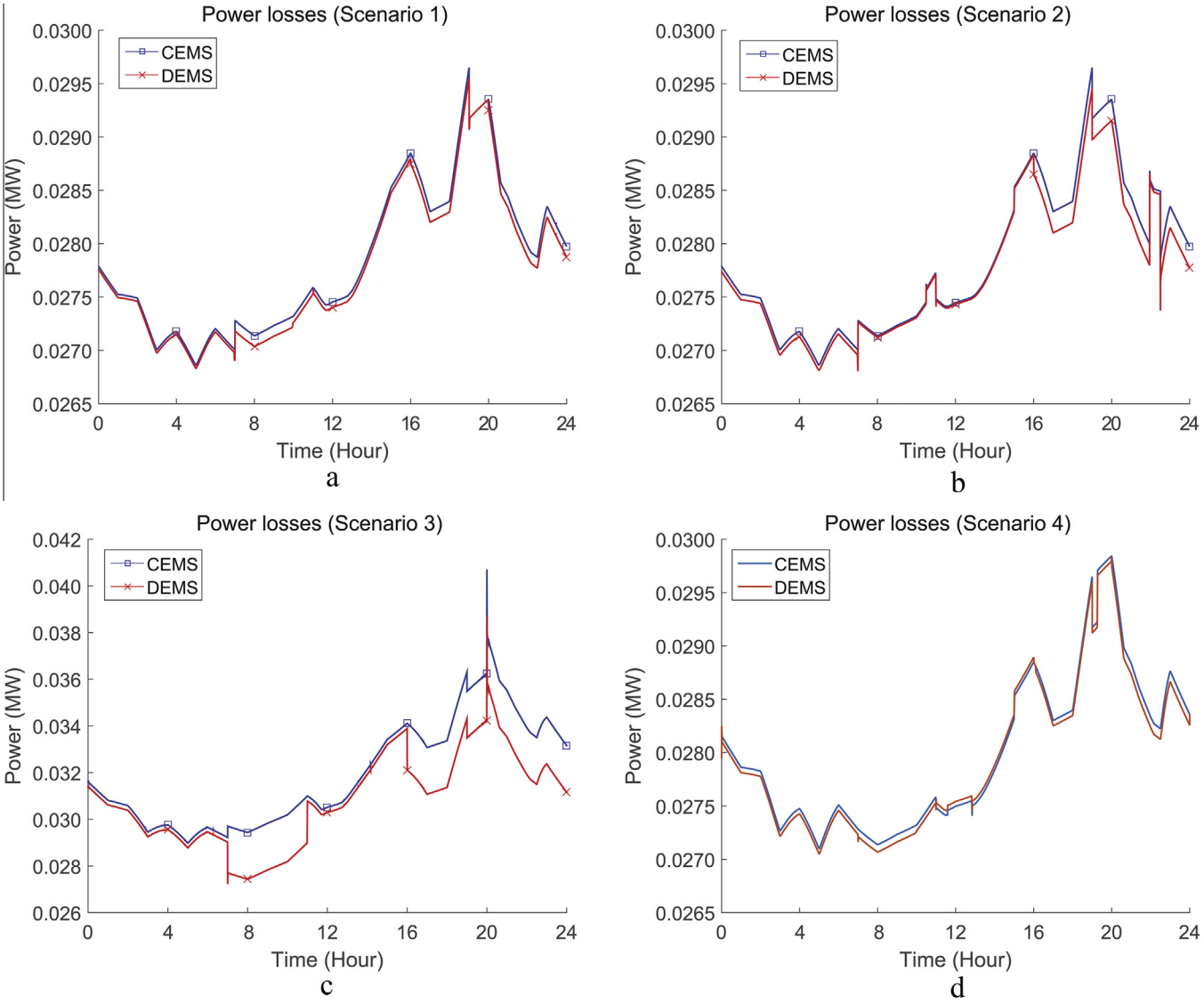

Fig. 32. Power losses for centralized EMS (CEMS) and distributed EMS (DEMS) (a) scenario 1, (b) scenario 2, (c) scenario 3 and (d) scenario 4.

$$\eta_{sys} = \frac{P_{Load}}{P_{RES} + P_{DG}} \tag{28}$$

where η_{sys} is the efficiency, P_{Load} is the total load, P_{RES} is the total power from renewable energy system, and P_{DG} is the total power from the diesel generation system. Furthermore, efficiency for each of the RE systems was also introduced which is defined as follows:

$$\eta_{PV} = \frac{P_{PV}}{P'_{PV}} \tag{29}$$

$$\eta_{wind} = \frac{P_{wind}}{P'_{wind}} \tag{30}$$

$$\eta_{hydro} = \frac{P_{hydro}}{P'_{hydro}} \tag{31}$$

where η_{pv} is the PV system efficiency, P_{PV} is the power generated form the PV system, P'_{PV} is the available solar power, η_{wind} is the wind system efficiency, P_{wind} is the power generated from the wind system, P'_{wind} is the available wind power, η_{hydro} is the hydropower system efficiency, P_{hydro} is the power generated form the hydropower system, and P'_{hydro} is the available hydropower. Furthermore, the microgrid performance was also evaluated based on the percentage of power losses in the system. The percentage of power losses, P_{loss} is calculated as follows:

$$P_{loss}(\%) = \frac{P_{RES} + P_{DG} - P_{load}}{P_{RES} + P_{DG}} \times 100 \tag{32}$$

In this study, the performance of the new multi-agent based EMS architecture has been compared to a conventional centralized EMS. The centralized EMS was built based on the typical centralized control topology, as shown in Fig. 1 and the control algorithm as in [2]. All constraints as in the distributed controller were implemented in the centralized controller, and all calculations were performed by a single centralized controller. In this paper, the algorithm implemented for the centralized controller is shown in Fig. 31.

In order to realize the comparison, both systems were simulated based on the same input parameters and disturbances. The EMS performances were evaluated based on efficiency parameters and power losses, and the results for each scenarios (S1, S2, S3 and S4) are listed in Table 6. Meanwhile, the comparison of the microgrid power losses between multi-agent based EMS and centralized EMS throughout the day for each scenario are shown in Fig. 32.

It is noticeable from the results that the centralized EMS has lower efficiency for each parameter compared to the multi-agent based EMS. This is due to MAS based EMS consists of agents that are distinct and unique to different types of energy sources and also distinct individually according to capacity, sizes and control algorithm. Therefore, it can provide faster controls than the corrective approach of conventional centralized control. The lower efficiency of centralized EMS also contributed by the computational burden of the centralized controller due to the extensive computation for performing optimization that later caused slow reaction time in handling the changes and disturbances that occurred in the microgrid.

7. Conclusion

This paper proposes a multi-agent based distributed control for handling complex energy management of a microgrid. In this paper, the proposed EMS architecture was presented alongside game theory implementation for multi agent coordination. There were seven agents introduced in the EMS representing each component of the microgrid. All microgrid components and agent models were developed and simulated in a Matlab/Simulink SimPowerSystems environment. In order to improve the microgrid performance, a new global objective function incorporating agent modes was introduced. Additionally, the primary facilitator was introduced in order to reduce flood of communication and streamline the decision making between agents. The proposed architecture was implemented in a case study microgrid. The EMS was simulated based on the selected site's real life renewable resources and load demand data. There were several scenarios such as resource fluctuations and load demand variations which were used to assess the EMS performance. Finally, the proposed multi-agent distributed control performances were compared to a centralized EMS based on efficiency parameters and power losses. The result shows that the proposed architecture has higher performance compared to the centralized EMS demonstrating its capability as a new energy management solution for a distributed hybrid energy generation system.

Acknowledgements

The author would like to thank the Ministry of Education (MOE), Malaysia, for funding this research under a FRGS research grant (20150214FRGS). The author would also like to thank the MOE for funding the corresponding author for PhD studies through the MyBrain15 (MyPhD) program.

References

[1] Ambia MN, Al-Durra A, Caruana C, Muyeen S. Power management of hybrid micro-grid system by a generic centralized supervisory control scheme. Sustain Energy Technol Assess 2014;8:57–65.
[2] Elsied M, Oukaour A, Gualous H, Hassan R. Energy management and optimization in microgrid system based on green energy. Energy 2015;84:139–51.
[3] Wang R, Wang P, Xiao G, Gong S. Power demand and supply management in microgrids with uncertainties of renewable energies. Int J Electr Power Energy Syst 2014;63:260–9.
[4] Kyriakarakos G, Dounis AI, Rozakis S, Arvanitis KG, Papadakis G. Polygeneration microgrids: a viable solution in remote areas for supplying power, potable water and hydrogen as transportation fuel. Appl Energy 2011;88:4517–26.
[5] Wang T, O'Neill D, Kamath H. Dynamic control and optimization of distributed energy resources in a microgrid; 2014. Available from arXiv preprint arXiv: 1410.0054.
[6] Olivares DE, Cañizares C, Kazerani M. A centralized optimal energy management system for microgrids. IEEE Power Energy Soc Gener Meet 2011:1–6.
[7] Jun Z, Junfeng L, Jie W, Ngan H. A multi-agent solution to energy management in hybrid renewable energy generation system. Renew Energy 2011;36:1352–63.
[8] Karavas C-S, Kyriakarakos G, Arvanitis KG, Papadakis G. A multi-agent decentralized energy management system based on distributed intelligence for the design and control of autonomous polygeneration microgrids. Energy Convers Manage 2015;103:166–79.
[9] Dou C-X, Wang W-Q, Hao D-W, Li X-B. MAS-based solution to energy management strategy of distributed generation system. Int J Electr Power Energy Syst 2015;69:354–66.
[10] Katiraei F, Iravani R, Hatziargyriou N, Dimeas A. Microgrids management. IEEE Power Energy Magaz 2008;6:54–65.
[11] Xu X, Jia H, Wang D, David CY, Chiang H-D. Hierarchical energy management system for multi-source multi-product microgrids. Renew Energy 2015;78:621–30.
[12] Torreglosa J, García P, Fernández L, Jurado F. Hierarchical energy management system for stand-alone hybrid system based on generation costs and cascade control. Energy Convers Manage 2014;77:514–26.
[13] Chang H-H. Genetic algorithms and non-intrusive energy management system based economic dispatch for cogeneration units. Energy 2011;36:181–90.
[14] Kyriakarakos G, Dounis AI, Arvanitis KG, Papadakis G. A fuzzy logic energy management system for polygeneration microgrids. Renew Energy 2012;41:315–27.
[15] Al-Saedi W, Lachowicz SW, Habibi D, Bass O. Power quality enhancement in autonomous microgrid operation using particle swarm optimization. Int J Electr Power Energy Syst 2012;42:139–49.
[16] Anh HPH. Implementation of supervisory controller for solar PV microgrid system using adaptive neural model. Int J Electr Power Energy Syst 2014;63:1023–9.

[17] Shoham Y, Leyton-Brown K. Multiagent systems: algorithmic, game-theoretic, and logical foundations. Cambridge University Press; 2008.
[18] Lagorse J, Paire D, Miraoui A. A multi-agent system for energy management of distributed power sources. Renew Energy 2010;35:174–82.
[19] Mocci S, Natale N, Pilo F, Ruggeri S. Demand side integration in LV smart grids with multi-agent control system. Electr Power Syst Res 2015;125:23–33.
[20] Rahman M, Mahmud M, Pota H, Hossain M. Distributed multi-agent scheme for reactive power management with renewable energy. Energy Convers Manage 2014;88:573–81.
[21] Logenthiran T, Srinivasan D, Khambadkone AM. Multi-agent system for energy resource scheduling of integrated microgrids in a distributed system. Electr Power Syst Res 2011;81:138–48.
[22] Vlassis N. A concise introduction to multiagent systems and distributed artificial intelligence. Synth Lect Artif Intell Mach Learn 2007;1:1–71.
[23] McArthur SD, Davidson EM, Catterson VM, Dimeas AL, Hatziargyriou ND, Ponci F, et al. Multi-agent systems for power engineering applications—part I: concepts, approaches, and technical challenges. IEEE Trans Power Syst 2007;22:1743–52.
[24] McArthur SD, Davidson EM, Catterson VM, Dimeas AL, Hatziargyriou ND, Ponci F, et al. Multi-agent systems for power engineering applications—part II: technologies, standards, and tools for building multi-agent systems. IEEE Trans Power Syst 2007;22:1753–9.
[25] Weiss G. Multiagent systems: a modern approach to distributed artificial intelligence. MIT press; 1999.
[26] Russell S, Norvig P. Artificial intelligence: a modern approach. New Jersey: Pearson Education International; 2003.
[27] Ingham J. What is an Agent. Centre for Software Maintenance, University of Durhan, Durhan, London Technical Report 6; 1997. p. 99.
[28] Fathima AH, Palanisamy K. Optimization in microgrids with hybrid energy systems – a review. Renew Sustain Energy Rev 2015;45:431–46.
[29] Tian H, Mancilla-David F, Ellis K, Muljadi E, Jenkins P. A cell-to-module-to-array detailed model for photovoltaic panels. Sol Energy 2012;86:2695–706.
[30] Wu K, Zhou H. A multi-agent-based energy-coordination control system for grid-connected large-scale wind–photovoltaic energy storage power-generation units. Sol Energy 2014;107:245–59.
[31] Khan B, Reyasudin M, Pasupuleti J, Jidin R. Micro-hydro and pico-hydro potential assessment for ungauged sites in the South China Sea islands. Applied mechanics and materials. Trans Tech Publ; 2015 [p. 632–6].
[32] Khan M, Jidin R, Pasupuleti J, Shaaya SA. Micro-hydropower potential assessment and generation volatility due to seasonal climate. In: IEEE international conference on power and energy (PECon); 2014. p. 371–6.
[33] Bosona T, Gebresenbet G. Modeling hydropower plant system to improve its reservoir operation. Int J Water Resour Environ Eng 2010;2(4):87–94.
[34] Achaibou N, Haddadi M, Malek A. Modeling of lead acid batteries in PV systems. Energy Proc 2012;18:538–44.
[35] Müller JP, Pischel M. The agent architecture inteRRaP: concept and application; 2011.
[36] Girault F, Stinckwich S. Footux team description a hybrid recursive based agent architecture. RoboCup-99: Robot Soccer World Cup III. Springer; 2000 [pp. 567–71].
[37] McGuire JG, Kuokka DR, Weber JC, Tenenbaum JM, Gruber TR, Olsen GR. SHADE: technology for knowledge-based collaborative engineering. Concurr Eng 1993;1:137–46.
[38] Rezaei N, Kalantar M. Hierarchical energy and frequency security pricing in a smart microgrid: an equilibrium-inspired epsilon constraint based multi-objective decision making approach. Energy Convers Manage 2015;98:533–43.
[39] Nguyen DT, Le LB. Optimal energy management for cooperative microgrids with renewable energy resources. In: IEEE international conference on smart grid communications (SmartGridComm); 2013. p. 678–83.
[40] Mei S, Wang Y, Liu F, Zhang X, Sun Z. Game approaches for hybrid power system planning. IEEE Trans Sustain Energy 2012;3:506–17.
[41] Khan MRB, Jidin R, Pasupuleti J, Shaaya SA. Optimal combination of solar, wind, micro-hydro and diesel systems based on actual seasonal load profiles for a resort island in the South China Sea. Energy 2015;82:80–97.
[42] Bruni G, Cordiner S, Mulone V. Domestic distributed power generation: effect of sizing and energy management strategy on the environmental efficiency of a photovoltaic-battery-fuel cell system. Energy 2014;77:133–43.